AN INVESTIGATION INTO THE CHARACTERISTICS OF THE EDGE MOUNTED COAXIAL TEM-LINE ANTENNA

Dale Edward Schultz

NAVAL POSTGRADUATE SCHOOL
Monterey, California

THESIS

AN INVESTIGATION INTO THE CHARACTERISTICS
OF
THE EDGE MOUNTED COAXIAL TEM-LINE ANTENNA

by

Dale Edward Schultz

Thesis Advisor: R.W. Adler

December 1972

Approved for public release; distribution unlimited.

An Investigation into the Characteristics of The Edge Mounted Coaxial TEM-line Antenna

by

Dale Edward Schultz
Lieutenant, United States Navy
B.S.E.E., University of Colorado, 1966

Submitted in partial fulfillment of the requirements for the degree of

MASTER OF SCIENCE IN ELECTRICAL ENGINEERING

from the

NAVAL POSTGRADUATE SCHOOL
December 1972

ABSTRACT

The edge mounted TEM-line antenna is a lightweight, low profile, medium-gain UHF-VHF traveling wave antenna. The antenna is capable of operating in several different modes in a given frequency band. In its simplest form the antenna consists of a small diameter semi-rigid coaxial transmission line bonded to the edge of a conducting ground plane. Sections of the coax outer conductor are removed at periodic intervals to form the radiating elements.

This paper presents methods of measuring and calculating the characteristic impedance and discontinuity capacitance of a single edge mounted radiating element. Scattering parameter techniques are employed to investigate input impedance and power absorption characteristics of arrays of TEM-line elements. Far-field radiation patterns are used to determine antenna gains and compare the performance of different array configurations.

TABLE OF CONTENTS

LIST OF FIGURES

30. Radiation patterns of the five gap antennas at 900 MHz
    (a) 5 cm gaps, 12 db above isotropic
    (b) 10 cm gaps, endfire lobe 3 db above isotropic ---------- 50

I. INTRODUCTION

A. DESCRIPTION OF ANTENNA

A TEM-line antenna is a low profile array of electrically small radiating elements distributed over a ground plane [1]. Electrically small means that the element length will not exceed one-quarter wavelength and in practice is usually smaller. The simplest form of the TEM-line antenna consists of a coaxial transmission line, at least 2 wavelengths long, with periodic interruptions or gaps in its outer conductor. Electrical continuity is maintained by bonding the coax to a conducting surface. Radiation occurs from the gaps by two radiation mechanisms, one due to current on the center conductor and the other due to the electric field between the center conductor and the ground plane called capacitor dipole radiation [2]. The structure derives its name from the principle propagating mode (Transverse electric and magnetic), which impinges on the gap from the coaxial line segments.

A TEM-line antenna constructed using .141" O.D. semi-rigid copper coax bonded to the edge of a ground plane is shown in Figure 1. The actual thickness of the ground plane is comparable to the diameter of the coax center conductor. This configuration has the physical properties of being lightweight, easily constructed, mechanically strong, and low profile. This edge mounted configuration can be completely flush mounted.

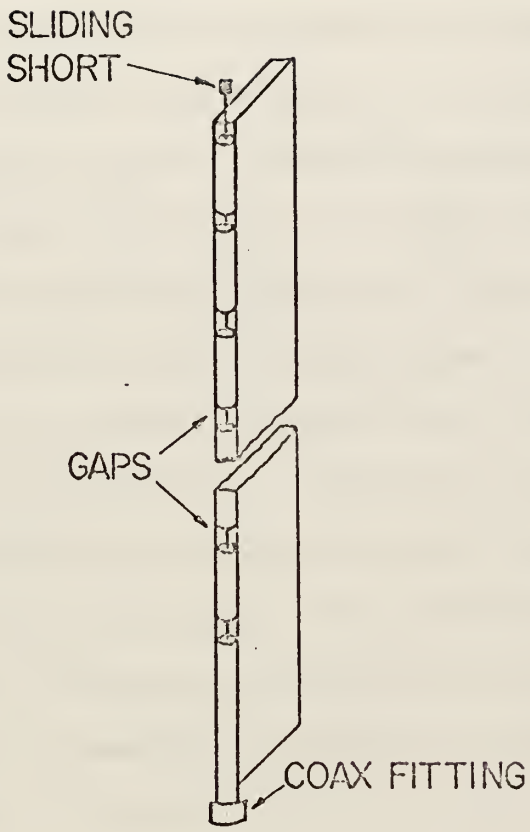

FIGURE 1. EDGE MOUNTED COAXIAL TEM-LINE ANTENNA

The TEM-line antennas, both the surface mounted and edge mounted versions, display a far field beam scanning characteristic whereby the beam position depends upon frequency. The beam scans from backfire to endfire as frequency increases. The number of beams in the far field pattern depends primarily on the gap spacing and the electrical termination of the structure. For optimum performance the structure is generally terminated in a short. The beam scanning characteristic of the antenna when terminated in a short and with typical one wavelength gap spacing is shown in Figure 2. The area of greatest interest in TEM-line antennas is the stopband region where the two beams merge and form a single broadside lobe. The broadside radiation condition persists over approximately 30% of the bandwidth before the beam again splits and continues scanning. It is in the stopband region that the greatest radiation efficiencies have been obtained and also the input impedance variation is somewhat less in this region than in others.

B. REVIEW OF RELATED WORK

Previous analysis of the TEM-line antenna, at Ohio State University, was done on the surface mounted and small loop versions of the antenna [1,2,3,4]. To simulate an antenna along the edge of a wing or fin, J. R. Copeland [4] attached the interrupted coax to the edge of the ground plane. The performance of this configuration was found to be generally similar to that of surface mounted TEM-line antennas, except

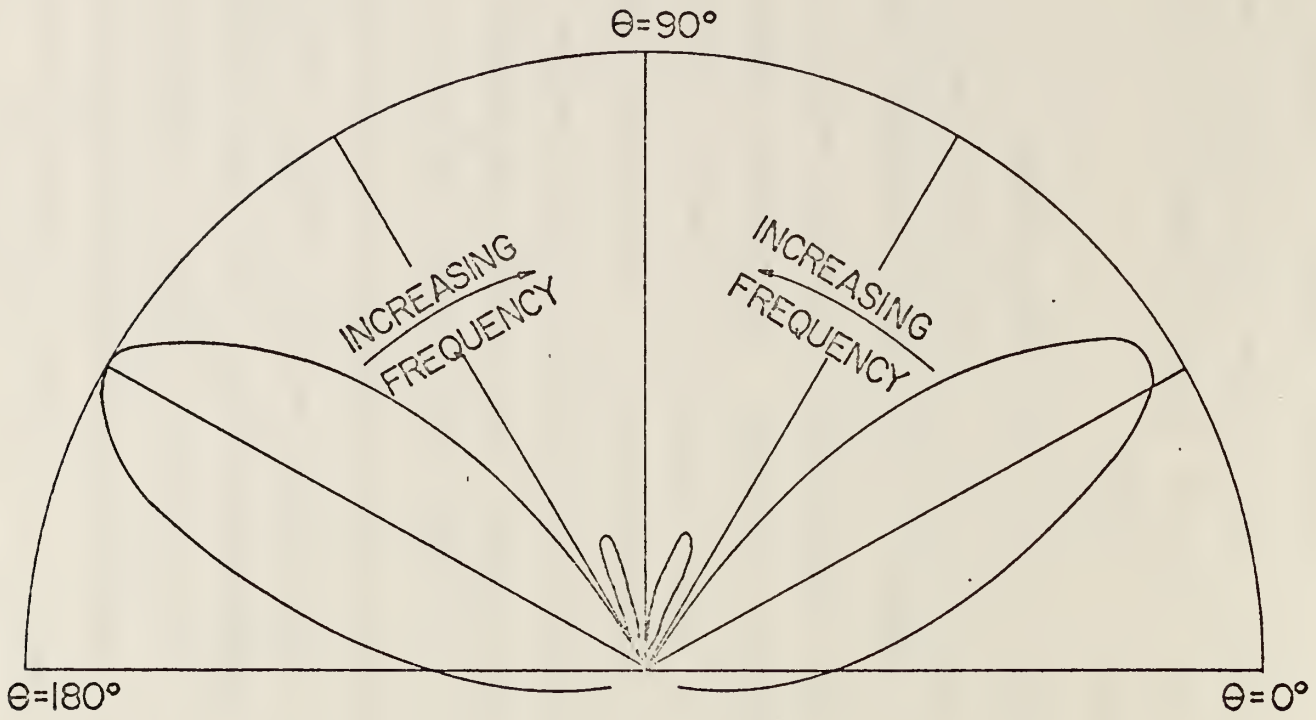

FIGURE 2. FAR FIELD RADIATION PATTERN FOR THE SURFACE MOUNTED TEM-LINE ANTENNA; SHORT CIRCUIT TERMINATION.

that the H-plane pattern was nearly a cardioid instead of the sinusoid obtained for the other cases. R. A Kitzerow did an analysis of a surface mounted TEM element and a four element TEM-line array [2]. In the analysis Kitzerow examined the impedance and radiation characteristics of both structures, developed equivalent circuits, and presented procedures for calculating component values of the circuits.

In a previous study done at the Naval Postgraduate School, J. N. Layl investigated the edge mounted version of the TEM-line antenna with the purpose of determining the impedance properties of a single edge mounted gap [5]. In the study Layl used time domain reflectometry and periodic structure theory to derive an equivalent circuit for the gap and to determine component values for one size gap. Layl also recorded far field radiation patterns of a five element edge mounted TEM-line structure. The patterns demonstrated the expected beam scanning and broad-side radiation characteristics of the antenna. Layl further achieved reasonably good results from the use of ω-β diagrams to predict operating characteristics of the five gap antenna.

C. STATEMENT OF PROBLEM

The first objective of this thesis is to further investigate the single edge mounted gap impedance properties to determine how the properties change as the gap length is changed. The basic edge mounted element is shown in Figure 3. This paper presents a method of measuring the impedance of

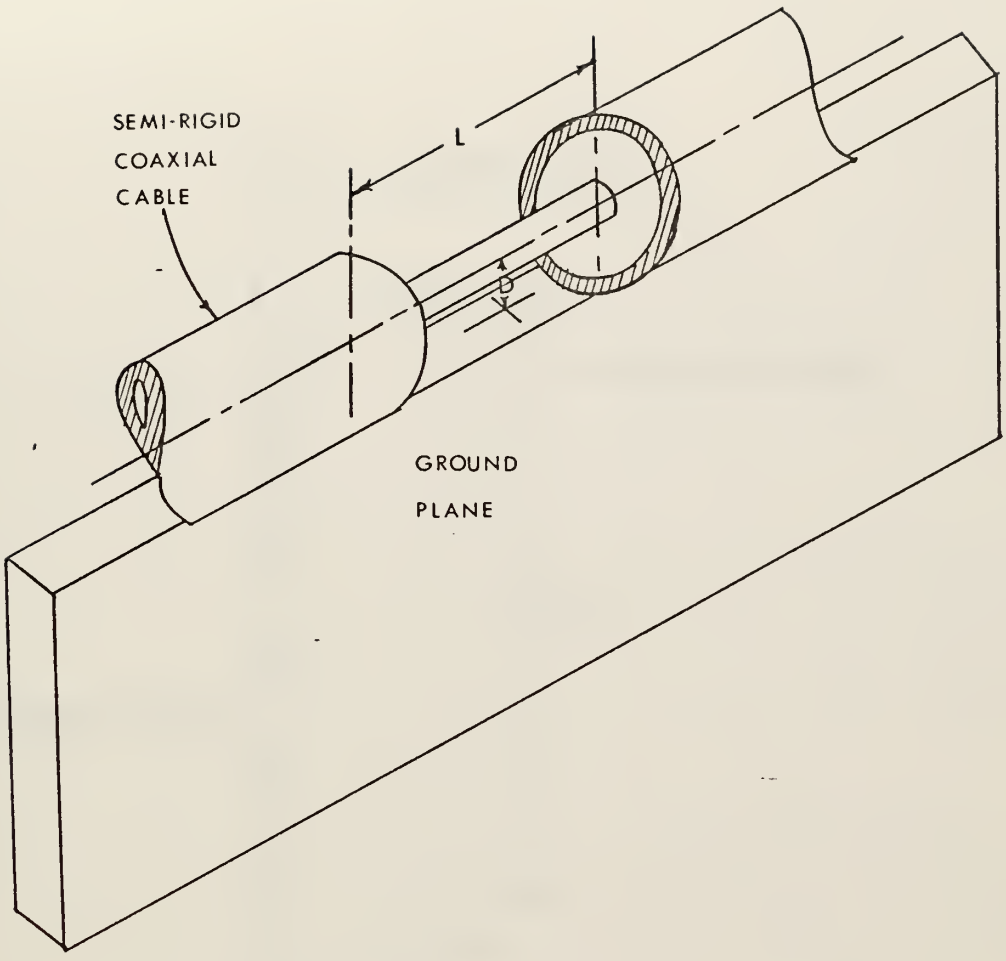

FIGURE 3. BASIC EDGE MOUNTED TEM-LINE RADIATING ELEMENT

any size gap, and discusses a means of calculating a gap characteristic impedance which will verify the measured values.

The second objective is to investigate the characteristics of an edge mounted array of elements as shown in Figure 4. Two structures with different size gaps were employed. Methods for determining the antenna input impedance, and the power radiating characteristics are discussed. Antenna

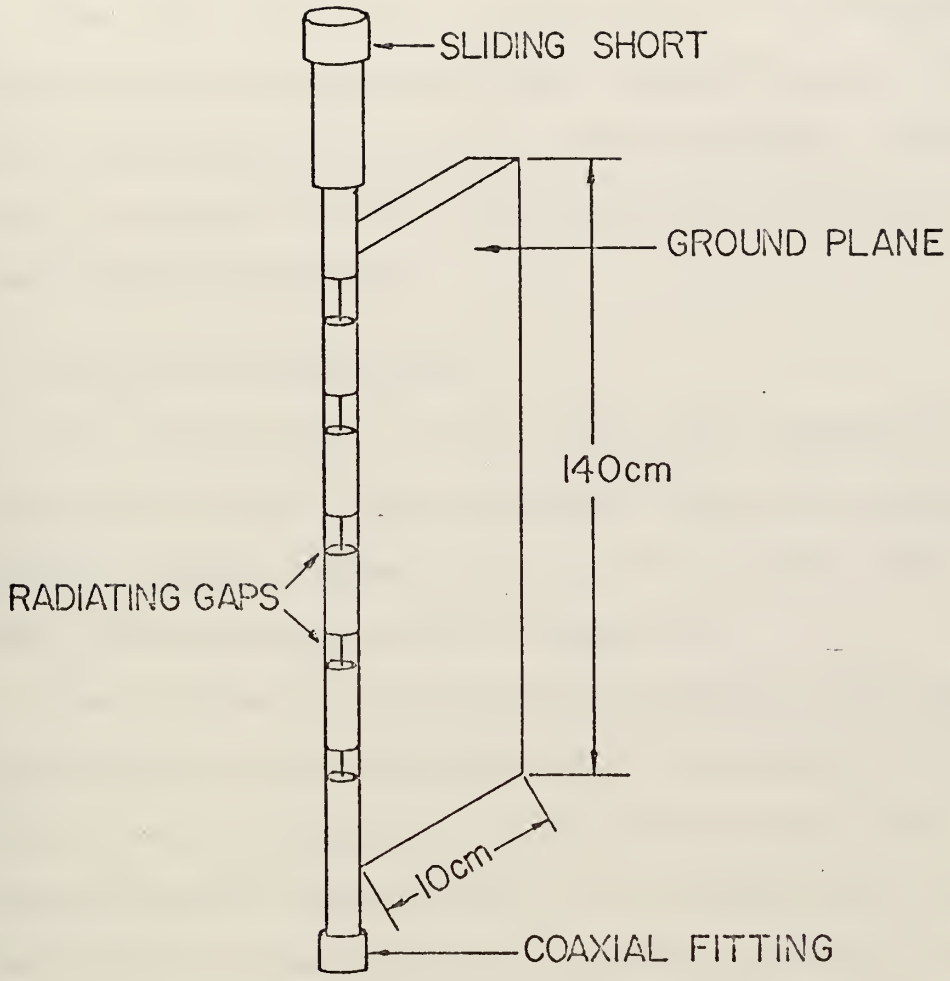

FIGURE 4. FIVE GAP EDGE MOUNTED COAXIAL TEM-LINE ANTENNA

far-field radiation pattern measurements were made to determine antenna gain, and further compare the performance of the two structures under investigation.

The final objective of this paper is to determine the utility of the edge mounted TEM structure as an antenna. This determination is based on the impedance, radiated power, pattern, and gain characteristics as measured on the two arrayed structures.

D. SCOPE AND LIMITATIONS

The investigation of the single gap impedance properties was carried out on five different single gap structures. The gap lengths ranged from 0.65 cm to 10 cm. The structures were constructed as shown in Figure 5.

The problem of single gap analysis was approached by assuming that the radiating center conductor and the ground plane form a transmission line section which has a constant characteristic impedance [2]. It is known that a change in transmission line geometry, in this case removal of the outer conductor, causes distortion of the electric and magnetic fields near the discontinuity. The distortion of the fields near the discontinuity is equivalent to shunting a small capacitance across the junction [6]. Thus a small discontinuity capacitance is required in the equivalent circuit that represents the impedance properties of an element. Figure 6 shows the approximate equivalent circuit for the single gap radiation and other loss resistances have been

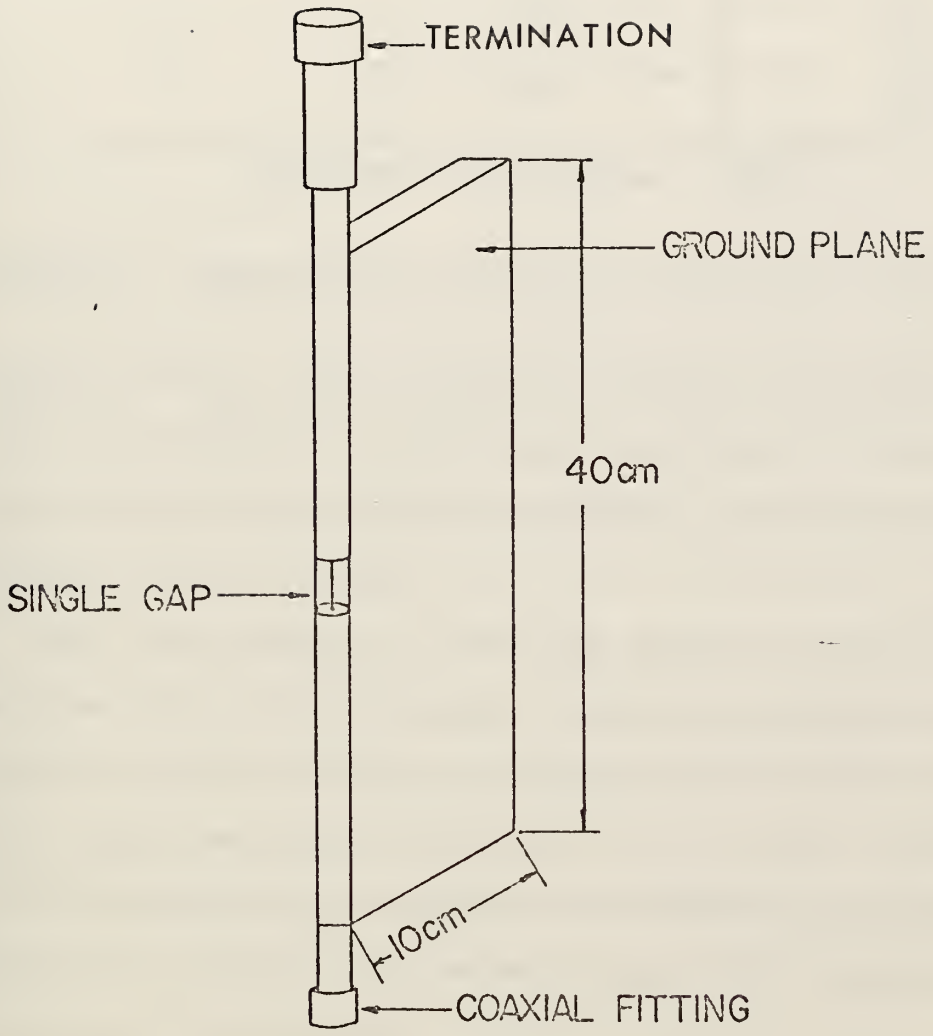

FIGURE 5. SINGLE GAP EDGE MOUNTED COAXIAL TEM-LINE ANTENNA

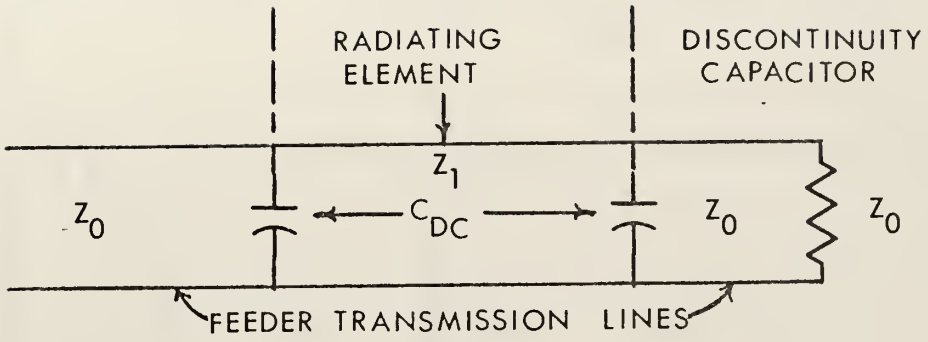

FIGURE 6. APPROXIMATE EQUIVALENT CIRCUIT OF A TEM-LINE ELEMENT

omitted because their values are assumed too small to affect these measurements. This study was limited to the determination of the characteristic impedance and the discontinuity capacitance for the gap.

The investigation of the edge mounted arrayed elements was done with two structures, as shown in Figure 4, with gap lengths of .125λ (5 cm) on one and 0.25λ (10 cm) on the other (gap length in wavelengths is at design frequency). The structures were designed for broadside operation at 750 MHz which required gap center to gap center spacing to be 0.7λ or 28 centimeters.

The TEM-line antenna can be considered as being composed of a number of individual cells connected in series. An individual cell consists basically of two transmission lines in tandem, one of which is the radiating element. A possible composite equivalent circuit of a cell is shown in Figure 7 [2]. R and G of the circuit are series resistance and shunt conductance accounting for energy loss by radiation and other

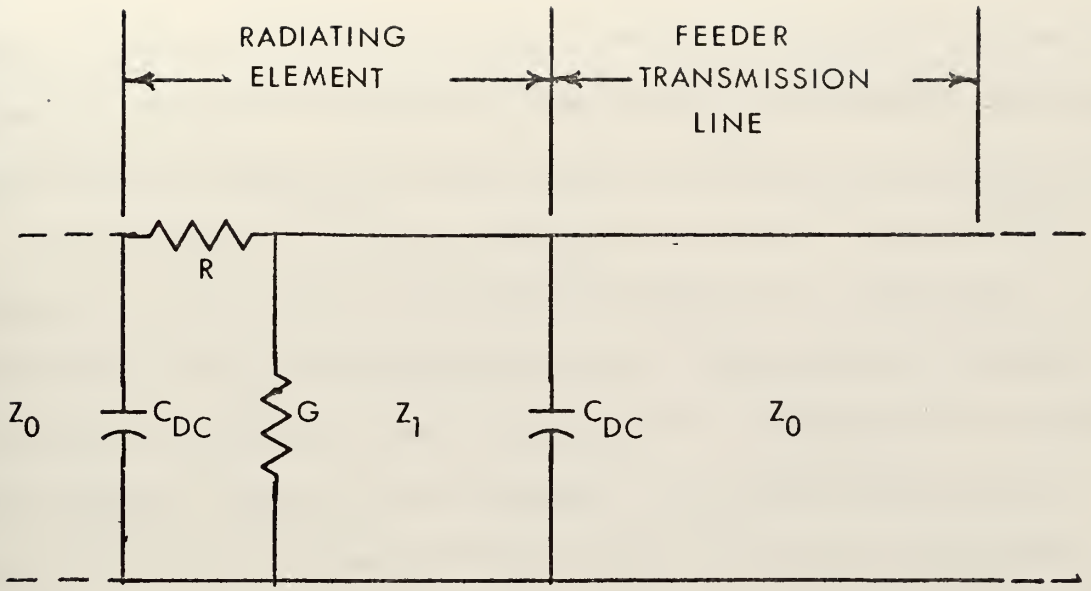

FIGURE 7. EQUIVALENT CIRCUIT OF A TEM-LINE ANTENNA CELL

mechanisms. The determination of values for R and G is beyond the scope of this study, but since the characteristics of the edge mounted antenna are very similar to the surface mounted version it is assumed that the values can be determined by methods similar to those established for the surface mounted antenna [2,3].

The antenna input impedance and power absorption characteristics were determined from scattering parameters as measured with a Vector Voltmeter. The accuracy of this technique is somewhat limited when the magnitude of a given s-parameter approaches one. Inherent in these measurements is a subtraction of the parameter from one. Subtracting two nearly equal numbers always results in a larger error in the difference than from the error in the parameter itself [7]. The situation is further complicated in the power computations because there the difference value is squared before it is

used. This limitation does not preclude meaningful results however, because accuracy in the power measurements was not required at frequencies where high reflections were present.

The number of antenna radiation patterns obtained was limited by the lengthy procedure required to impedance match and tune the antenna each time frequency was changed. Impedance matching is more difficult at frequencies outside the stopband than in the stopband. The matching problem restricted the accuracy of the gain and some of the power measurements made at frequencies outside the stopband, but since the stopband areas are the areas of greatest interest on these structures the restriction has little effect on the overall result of this study.

II. MEASUREMENTS AND RESULTS

A. IMPEDANCE CHARACTERISTICS OF A SINGLE EDGE MOUNTED TEM-LINE ELEMENT

As previously stated the gap can be interpreted as a transmission line segment with a constant characteristic impedance, and represented by an equivalent circuit as shown in Figure 6.

Time Domain Reflectometry (TDR) was used to measure the gap characteristic impedance. The particular TDR technique employed was the use of TDR as applied to cable testing [8]. This TDR technique employs the fact that a cable fault will show up as a positive or negative bump on the otherwise flat TDR oscilloscope presentation. A positive bump, as was observed on all gap measurements, means either that the characteristic impedance of the line is high over a short section or that there is a series inductance at a point in the line. If the discontinuity is flat-topped, as shown in Figure 8, it is best to treat it as a section of higher

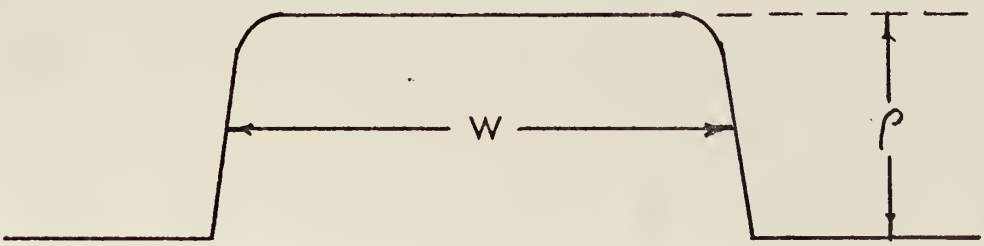

FIGURE 8. TDR DISPLAY OF A SHORT LENGTH OF COAX CABLE HAVING AN INCREASED Z DISCONTINUITY.

impedance cable with the impedance value given by $Z_1 = Z_o \frac{1 + \rho}{1 - \rho}$, Z_o is the feeder line impedance and ρ is measured as shown in Figure 8. The flat-topped discontinuity was observed for all gap sizes greater than 2.5 cm. The measured gap characteristic impedance as a function of gap length is shown in Figure 9.

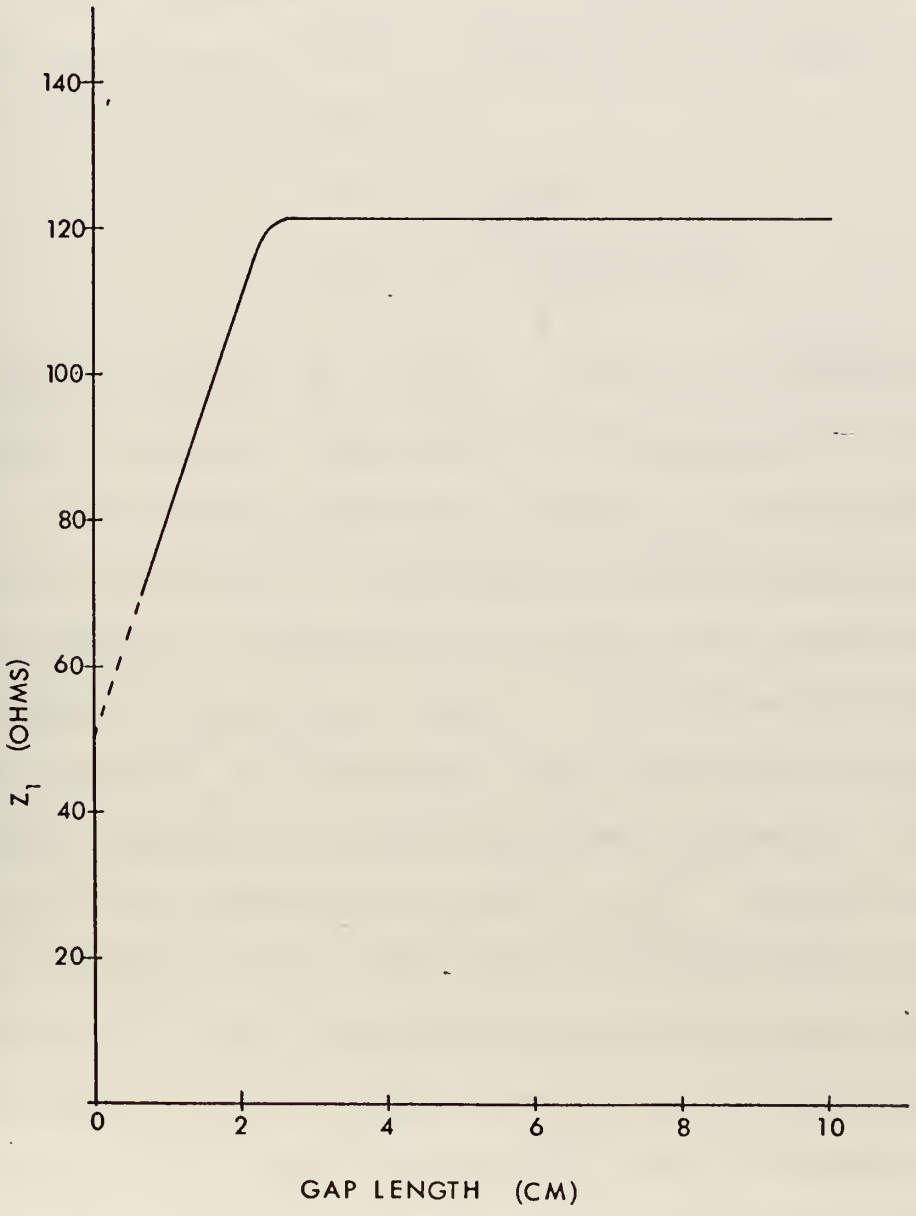

FIGURE 9. MEASURED GAP CHARACTERISTIC IMPEDANCE VERSUS GAP LENGTH.

The decrease in impedance as gap length decreases below 2.5 cm is attributed to the discontinuity capacitance C_{DC}. It will be shown that as the gap length decreases the value of C_{DC}, a constant for all of the gaps, approaches the value of the gap capacitance thus decreasing the characteristic impedance.

From transmission line theory gap characteristic impedance is found by (1) $Z_1 = \sqrt{L/C}$ and the phase velocity in the gap is given either by

$$(2) \quad v_p = \frac{1}{\sqrt{LC}} \quad \text{or}$$

$$(3) \quad v_p = \frac{3 \times 10^8 \text{ m/s}}{\sqrt{\varepsilon_r}}$$

from (1) and (2) $Z_1 = \frac{1}{Cv_p}$, where the capacitance C is in farads per meter. Therefore by determining the capacitance and the relative dielectric constant ε_r of the gap Z_1 is easily calculated. The value of ε_r was determined from TDR measurements of impedance as follows; the impedance of a 5 cm gap, with the coax dielectric on the center conductor, was measured, the dielectric was then removed from the center conductor and the measurement repeated. The ratio of the two impedances is equal to $\sqrt{\varepsilon_r}$, and the results indicate $\sqrt{\varepsilon_r} = 1.2$. The value of capacitance for the gap configuration was determined by field mapping techniques as explained by Hayt [9]. The gap capacitance was calculated to be C = 32.1 pF/m. Knowing $\sqrt{\varepsilon_r}$ and C the gap phase velocity and characteristic impedance were determined to be 2.5×10^8 m/s and 125 ohms respectively. Table I shows the value of gap capacitance for each gap.

TABLE I

Calculated Values of Gap Capacitance Versus Gap Length

Gap Length (CM)	Capacitance pF
0.65	0.208
1.3	0.418
2.5	0.805
5.0	1.60
10.0	3.21

The value of the discontinuity capacitance C_{DC} was determined from the measured impedance, on the smaller gaps, and the individual gap capacitance by:

$$C_T = \frac{l}{Z_l v_p}$$, where C_T = gap capacitance (Cg) + discontinuity capacitance (C_{DC}), therefore

$$C_{DC} = \frac{l}{Z_l v_p} - Cg$$ and the value calculated is C_{DC} = 0.16 pF. This value is the total discontinuity capacitance of a gap.

B. CHARACTERISTICS OF THE PERIODIC FIVE-ELEMENT EDGE-MOUNTED TEM-LINE ANTENNA

A possible equivalent circuit of a TEM-line antenna cell has been shown in Figure 7. The values of C_{DC} and Z_l are determined by methods described for the single gap. The total equivalent circuit of an N element antenna is obtained by adding N cells in series. The input to the first cell is

the feed end of the antenna, and the last cell is terminated in some arbitrary load impedance.

Scattering parameter techniques [10] were used for the measurement of array input impedance and power radiating characteristics. The magnitude and phase of the scattering matrix elements, s-parameters, were measured with a vector voltmeter as shown in Figure 10. The vector volt-meter provides both the magnitude and phase by measuring a voltage ratio and a phase difference [11], thus the s-parameters are determined by:

$$S_{11} = \frac{b_1}{a_1} \angle \phi_{b_1} - \phi_{a_1} \quad \text{and}$$

$$S_{21} = \frac{b_2}{a_2} \angle \phi_{b_2} - \phi_{a_2} \quad \text{where}$$

$a_1 = \frac{E_{i1}}{\sqrt{Z_o}}$ is the normalized incident wave on port 1,

$b_1 = \frac{E_{r1}}{\sqrt{Z_o}}$ is the normalized reflected wave at port 1, a_2 and b_2 are similar values at port 2, S_{11} is the reflection coefficient looking into port one, and S_{21} is the transmission coefficient from port 1 to port two [10]. The antennas are symmetric two port devices where $S_{11} = S_{22}$ by symmetry and $S_{12} = S_{21}$ by reciprocity; thus only two of the four scattering matrix elements need to be measured to obtain all necessary information for impedance and power calculations.

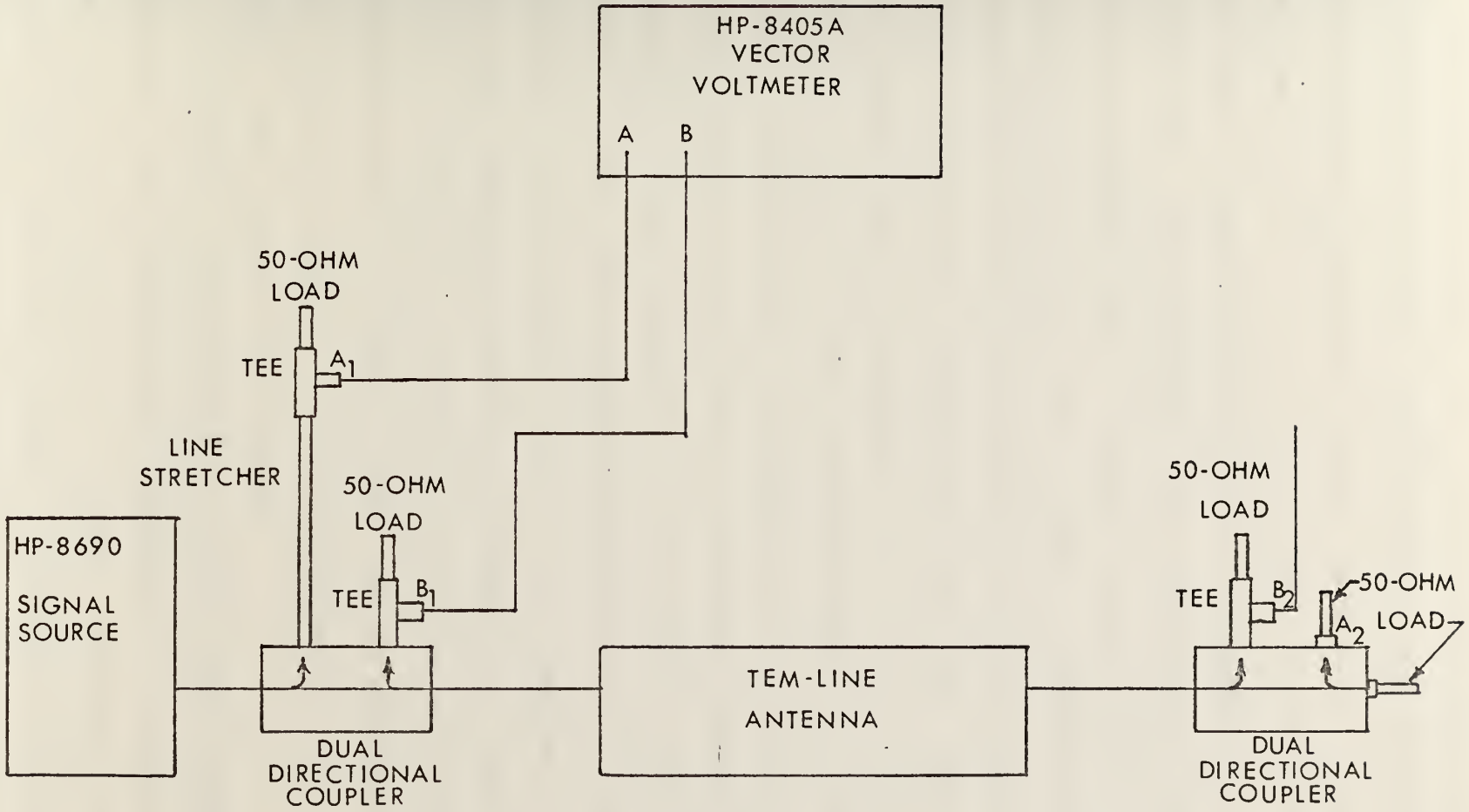

FIGURE 10. EQUIPMENT SET-UP FOR S-PARAMETER MEASUREMENTS

The measured value of S_{11} is the reflection coefficient ρ, magnitude and phase, at the input to the structure. The antenna input impedance is easily determined by plotting the measured value of ρ on the Smith chart, and then rotating the point an amount equivalent to the length of the input feeder line. The normalized input impedance is then read directly from the chart. The Smith chart plot of input impedance for the array of 5 cm gaps is shown in Figure 11. These plots represent the impedance at the junction of the feeder transmission line with the first gap. The plots show two regions where the magnitude of the input impedance is high; the first is in the invisible region [3] and the second is the stopband region. The magnitude of the input impedance of the antenna can be taken as a relative measure of the magnitude of the impedance at each element. This general trend will be useful in explaining some of the radiation patterns. Polar plots of the real and imaginary parts of the input impedance are shown in Figure 12. These plots further demonstrate the regions where the magnitude of the input impedance is high, and show the varying magnitude as the frequency changes. Of particular note is the high value at the upper end of the stopband.

To further investigate the antenna input impedance characteristics the structure was terminated in a moveable short and the input impedance, at a given frequency, was observed as the short was moved through a distance of one-half wavelength. The impedance variation is shown on Smith Chart

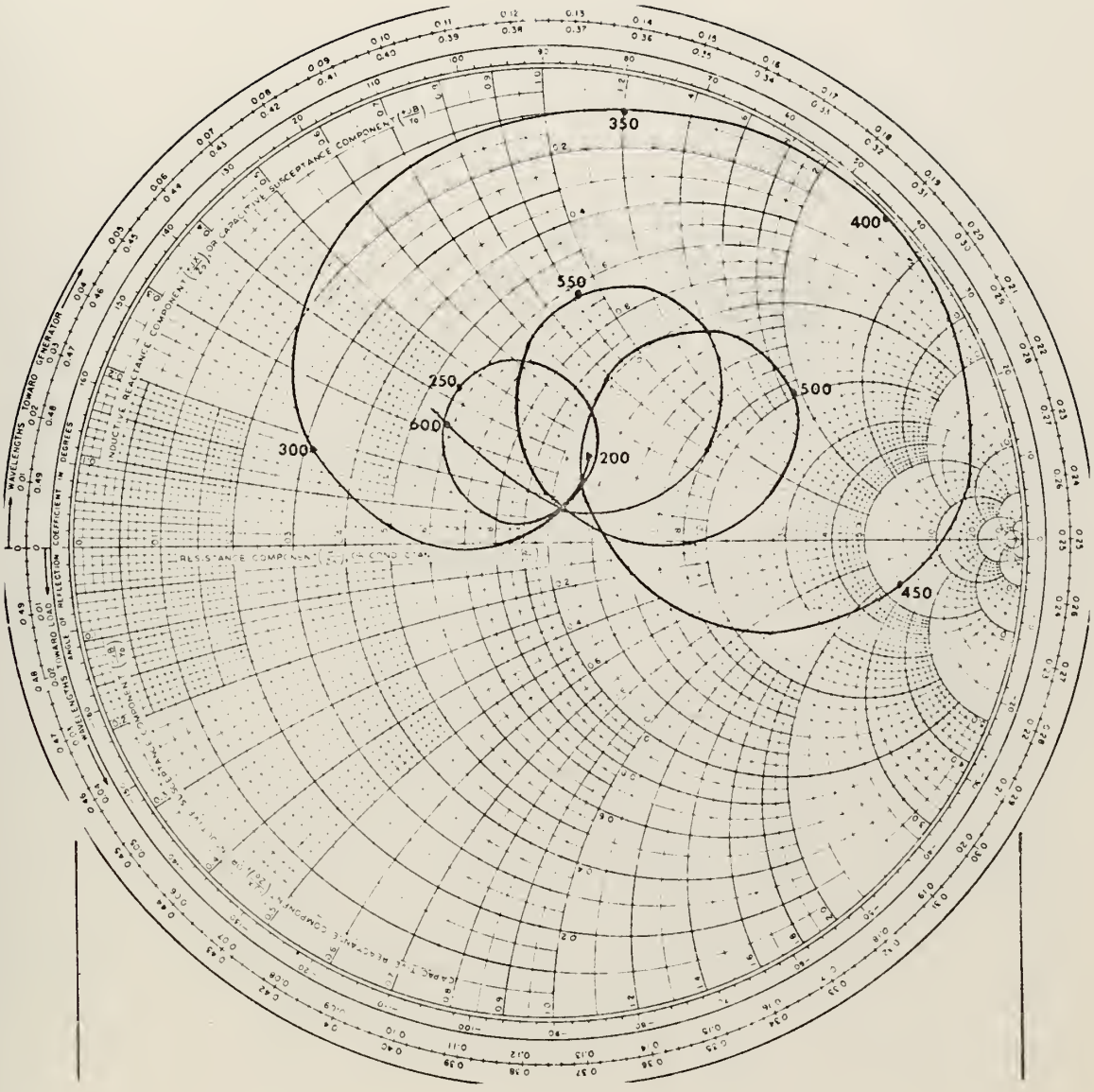

FIGURE 11a. INPUT IMPEDANCE OF A FIVE-ELEMENT EDGE MOUNTED TEM-LINE ANTENNA TERMINATED IN A 50 OHM LOAD (200 MHz - 600 MHz).

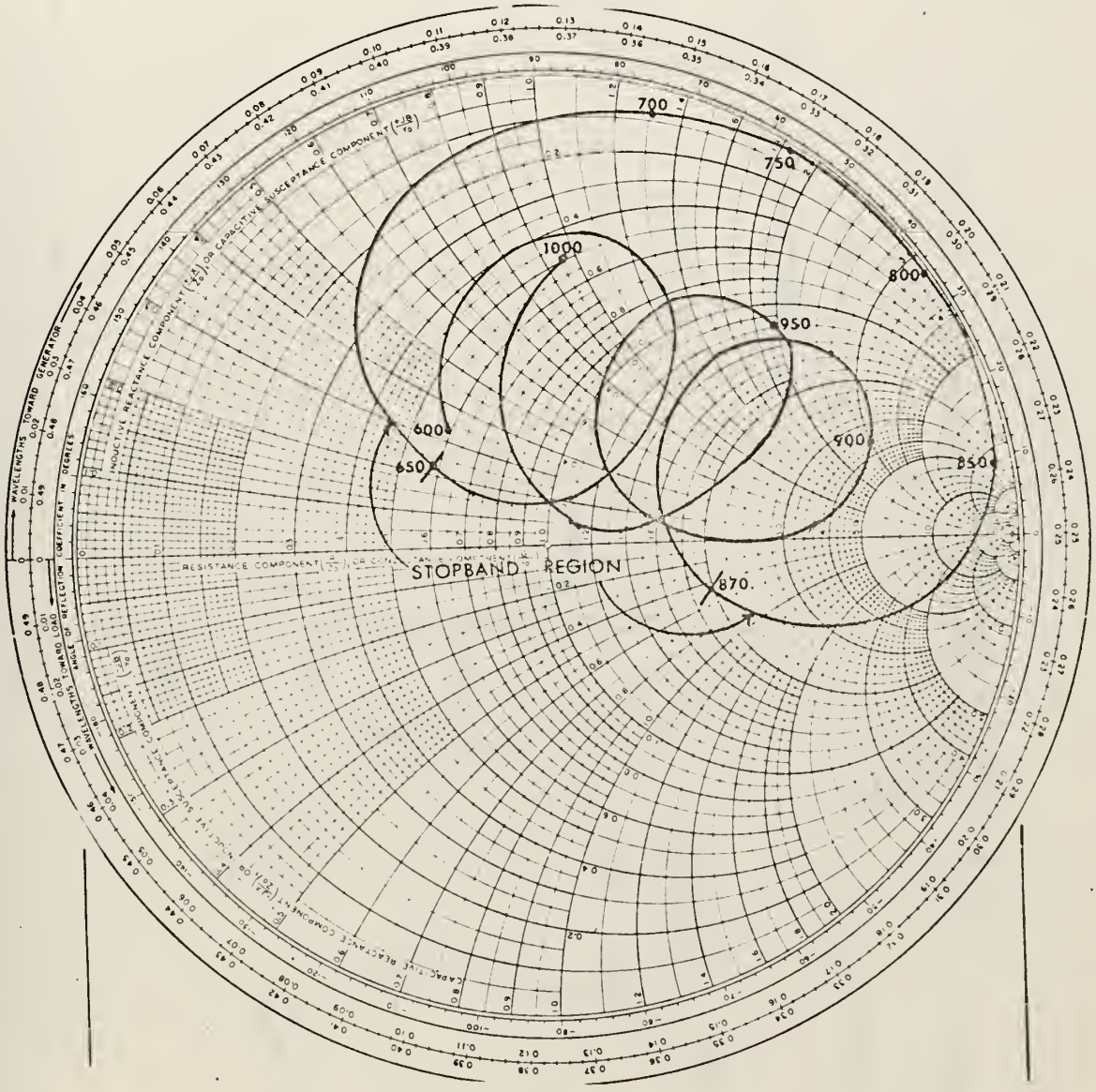

FIGURE 11b. INPUT IMPEDANCE OF A FIVE-ELEMENT EDGE MOUNTED TEM-LINE ANTENNA TERMINATED ON A 50 OHM LOAD (600 MHz - 1000 MHz).

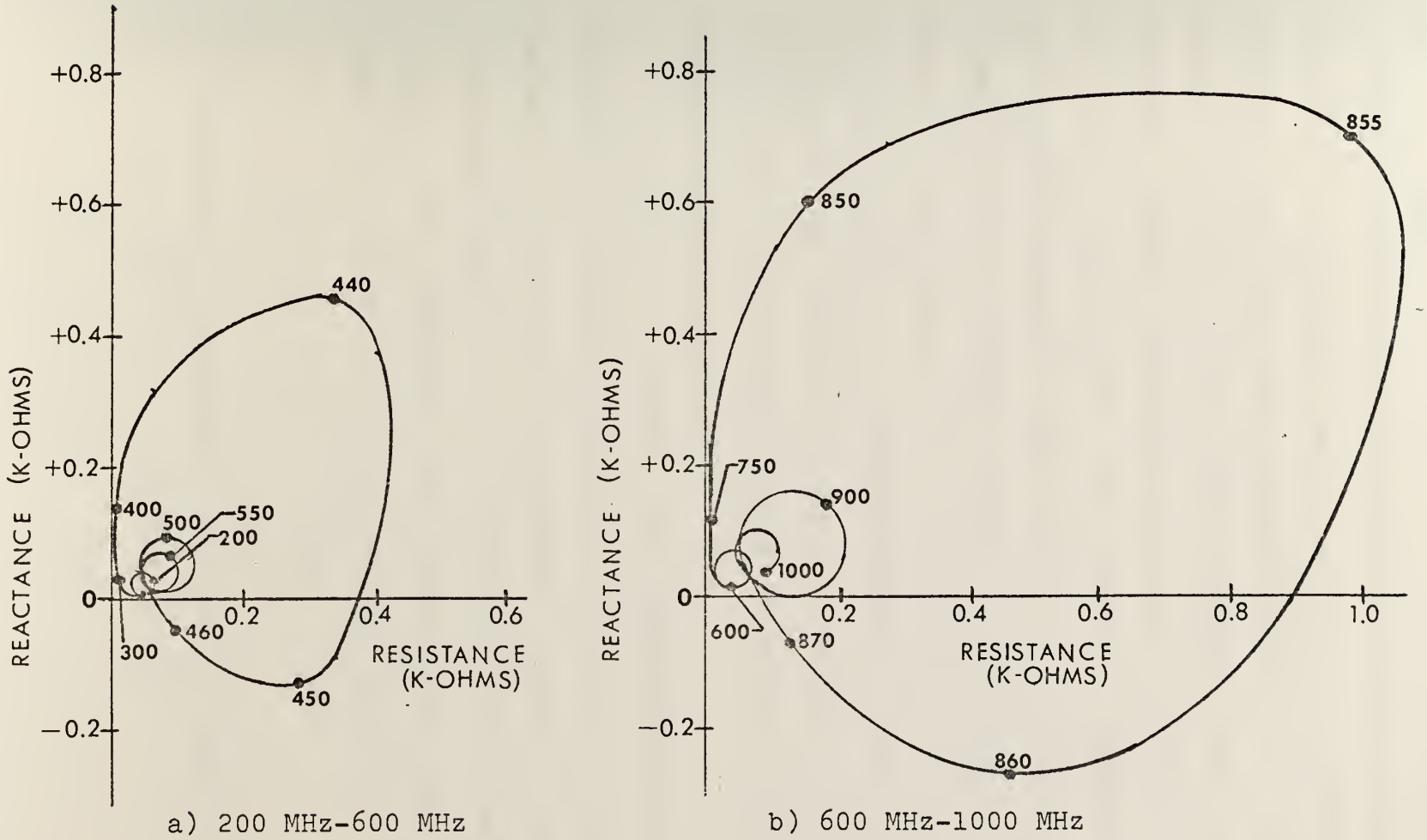

a) 200 MHz-600 MHz

b) 600 MHz-1000 MHz

FIGURE 12. INPUT IMPEDANCE OF THE FIVE-ELEMENT ANTENNA AS A FUNCTION OF FREQUENCY

plots in Figures 13 through 18. A wide impedance variation is noted at frequencies above and below the stopband, Figures 13 and 16. A somewhat smaller variation is observed at frequencies just inside the stopband, Figure 15. And as demonstrated in Figure 14, the input impedance, for all practical purposes, was not effected by the short position at frequencies inside the stopband. The effect of impedance matching at the input, when the short is in the zero position, is demonstrated by comparing Figure 14 with Figure 17 and Figure 16 with Figure 18. At frequencies inside the stopband the input essentially remained matched as the short position changed while outside the stopband the match only occured at the zero position and at short positions corresponding to half-wavelength intervals.

As previously described, all information necessary for determining impedance and power is available from the measurement of two of the s-parameters, namely S_{11} and S_{21}. The method derived for calculating the power characteristics from the two parameters is as follows. The two reflected waves are related to the two incident waves by:

$$(1)\quad b_1 = S_{11}a_1 + S_{12}a_2 \qquad \text{and}$$

$$(2)\quad b_2 = S_{21}a_1 + S_{22}a_2.$$

If the device is terminated as shown in Figure 10, then $a_2 = 0$ and equations (1) and (2) become

$$(3)\quad b_1 = S_{11}a_1 \qquad \text{and}$$

$$(4)\quad b_2 = S_{21}a_1.$$

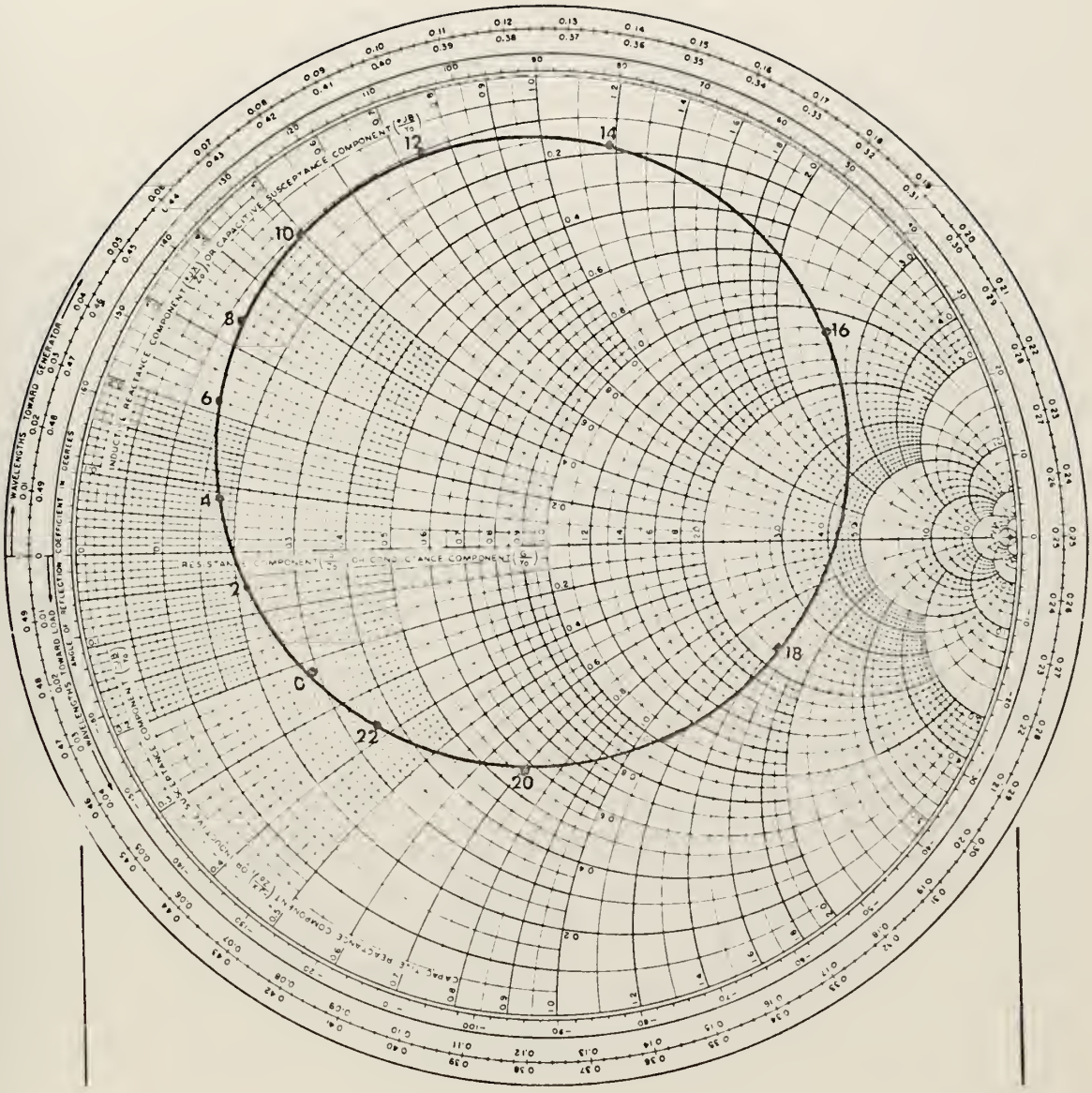

FIGURE 13. INPUT IMPEDANCE OF THE FIVE-ELEMENT ANTENNA SHOWING THE EFFECTS OF THE ADJUSTABLE SHORT TERMINATION, 650 MHz.

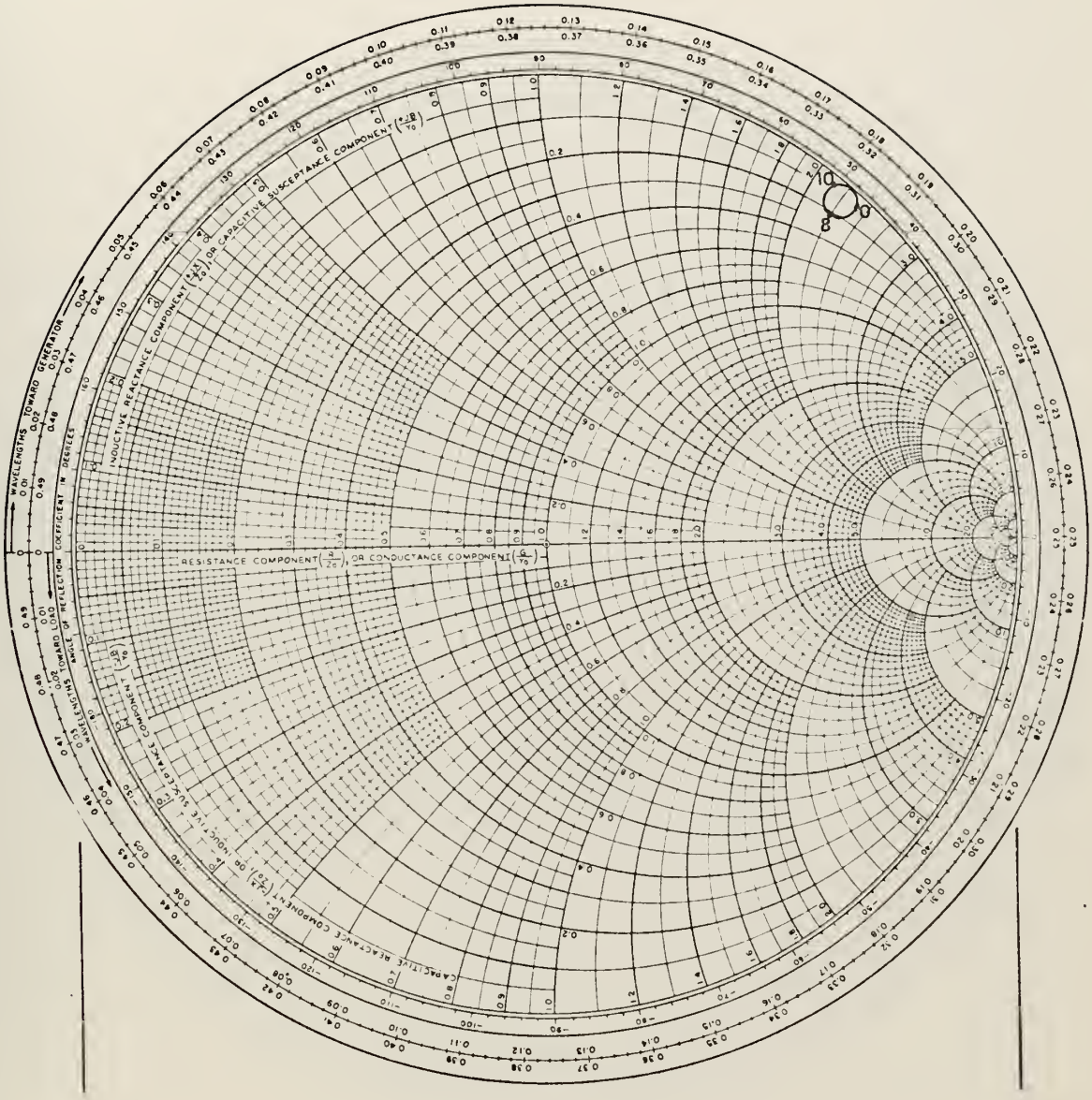

FIGURE 14. INPUT IMPEDANCE OF THE FIVE-ELEMENT ANTENNA SHOWING THE EFFECTS OF THE ADJUSTABLE SHORT TERMINATION, 750 MHz.

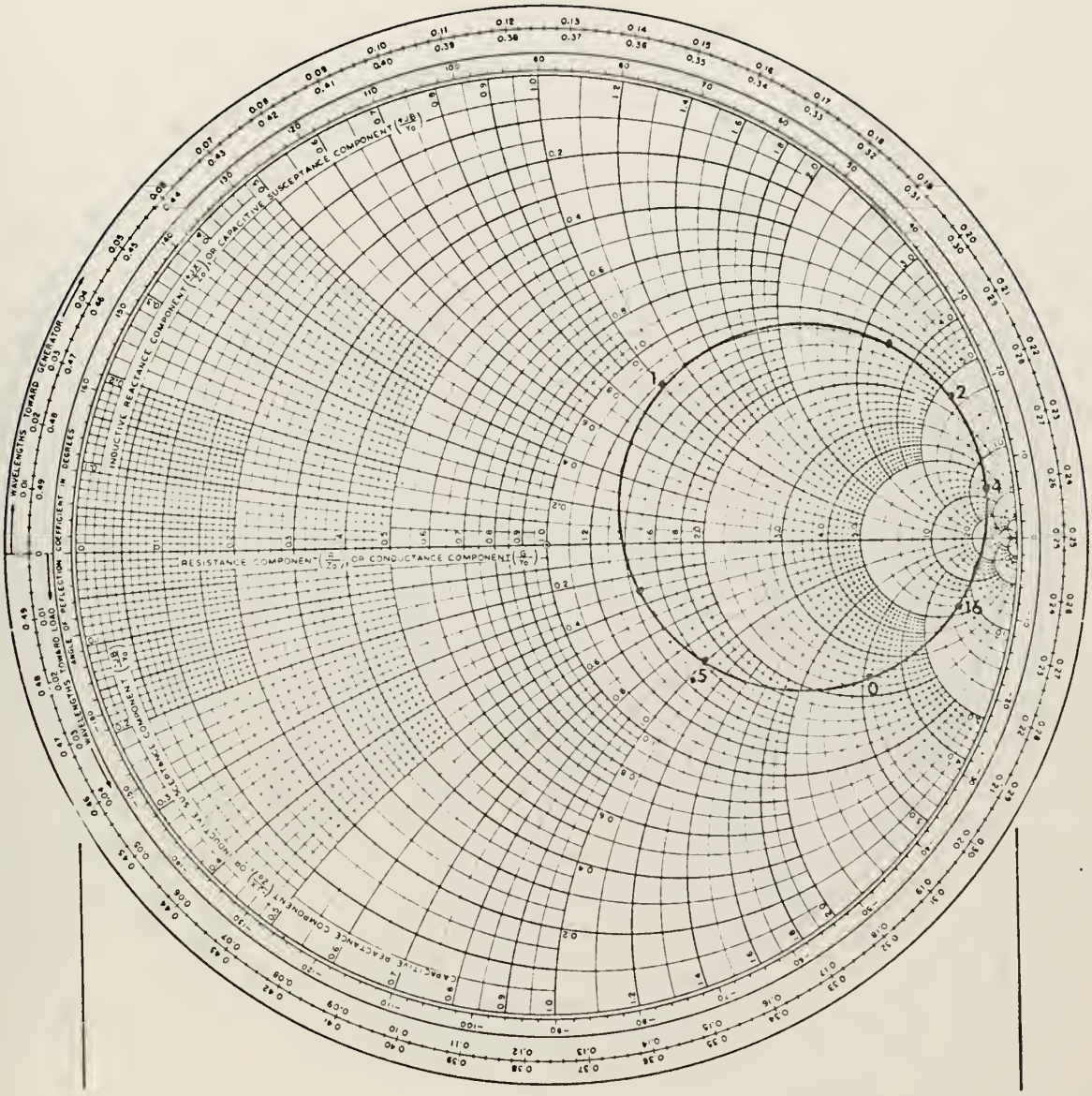

FIGURE 15. INPUT IMPEDANCE OF THE FIVE-ELEMENT ANTENNA SHOWING THE EFFECTS OF THE ADJUSTABLE SHORT TERMINATION, 850 MHz.

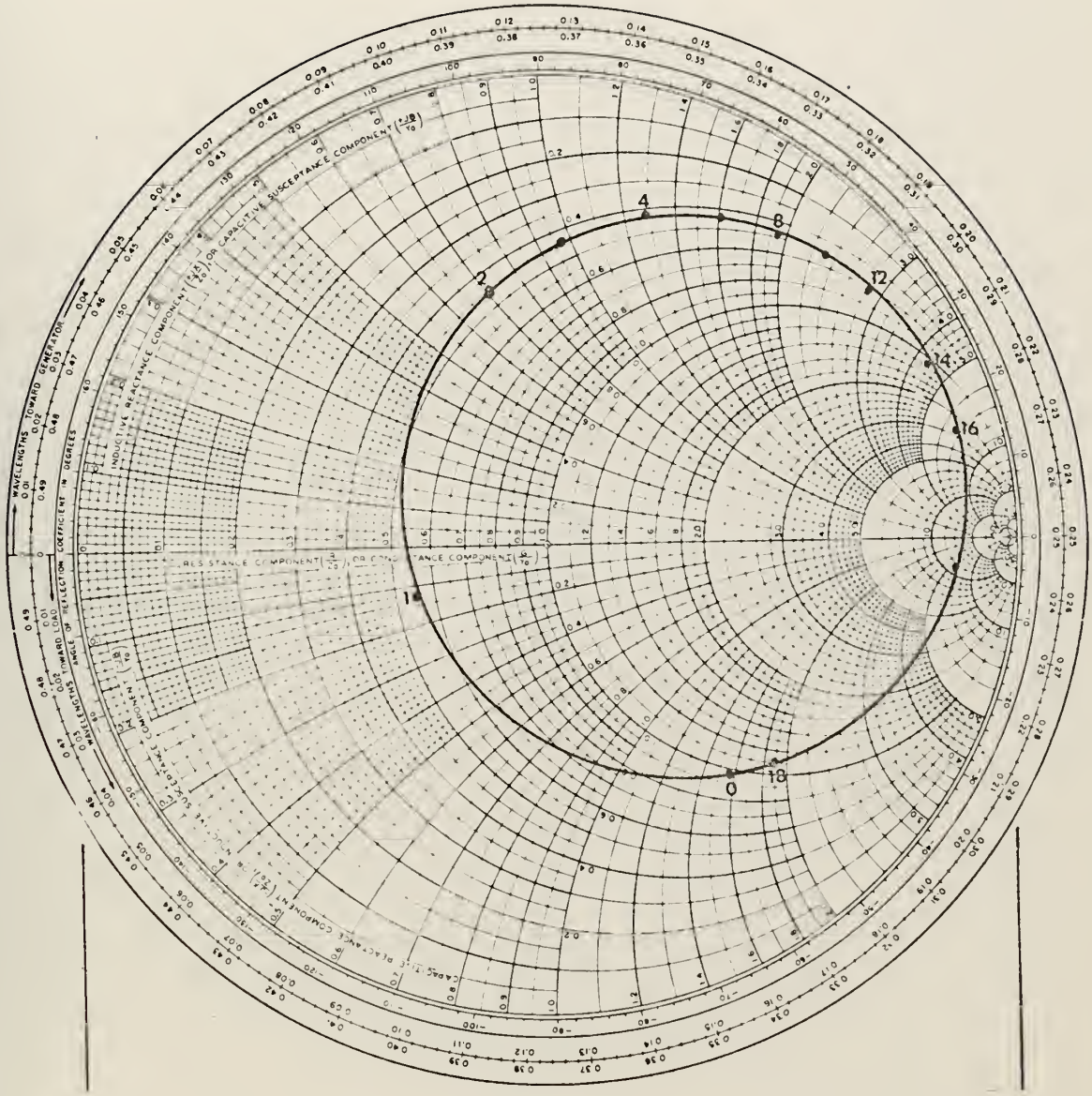

FIGURE 16. INPUT IMPEDANCE OF THE FIVE-ELEMENT ANTENNA SHOWING THE EFFECTS OF THE ADJUSTABLE SHORT TERMINATION, 875 MHz.

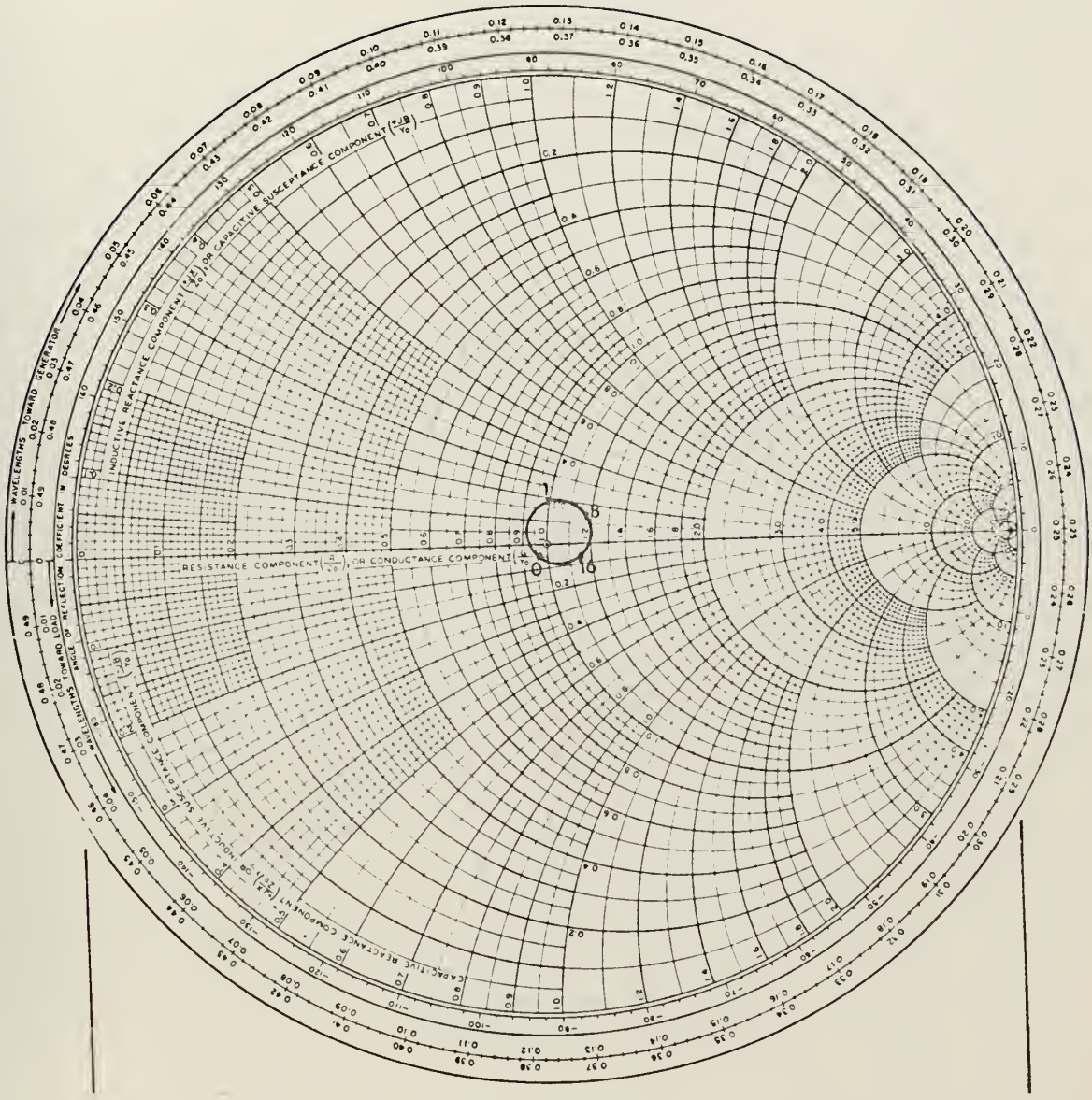

FIGURE 17. INPUT IMPEDANCE SHOWING THE EFFECTS OF THE ADJUSTABLE SHORT TERMINATION, INPUT MATCHED AT THE ZERO SHORT POSITION, 750 MHz.

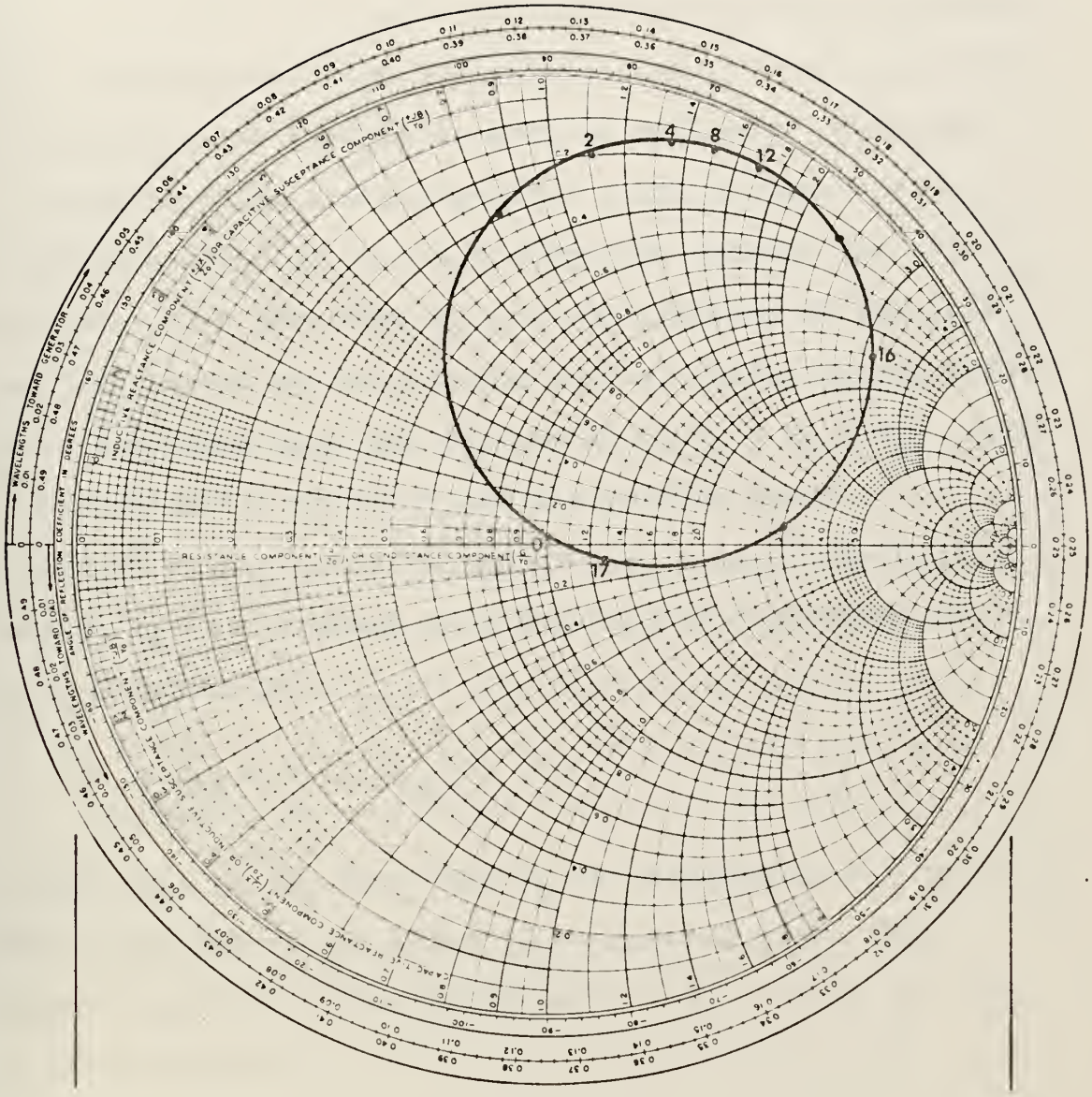

FIGURE 18. INPUT IMPEDANCE SHOWING THE EFFECTS OF THE ADJUSTABLE SHORT TERMINATION, INPUT MATCHED AT THE ZERO SHORT POSITION, 875 MHz.

Using the expressions for the normalized waves it can be shown [10] that $|a_1|^2$ is the incident or input power to the structure (P_i), $|b_1|^2$ is the reflected power from port one (P_r), and $|b_2|^2$ is the power transmitted through the antenna (P_o). To show the characteristics of the antenna, by power calculations, two quantities must be defined. Power lost (P_L) is defined as non-transmitted power or the fraction of the input power that is not transmitted through the structure, and power absorbed (P_a) is the fraction of the input power dissipated on the antenna through radiation and ohmic loss. The power lost was determined by $P_L = P_i - P_o$. From the definition of incident and transmitted power $P_L = |a_1|^2 - |b_2|^2$, then using (4), $P_L = |a_1|^2 [1-|S_{21}|^2]$. Finally, P_L is expressed as a fraction or percentage of the input power by

$$\frac{P_L}{|a_1|^2} = (1 - |S_{21}|^2)\ 100.$$

Of note here is the fact that P_r is included in P_L; that is, power reflected at the input is considered lost. The absorbed power is determined from $P_a = P_i - (P_r + P_o)$ and can be written as

$$P_a = |a_1|^2 - |b_1|^2 - |b_2|^2 \quad \text{or}$$

$$P_a = |a_1|^2 (1 - |S_{11}|^2 - |S_{21}|^2) \quad \text{and finally}$$

$$\frac{P_a}{|a_1|^2} = (1 - |S_{11}|^2 - |S_{21}|^2)\ 100 \quad \text{is the}$$

percentage of input power absorbed on the antenna.

Figure 19 shows P_L and P_a at frequencies between 200 and 1000 MHz, for the 5 cm gap antenna, with the antenna input unmatched. The plot of P_L again shows the stopband region where practically all of the incident power is reflected due to the high input impedance. The stopband region as seen here extends over the same frequency range as indicated in Figure 11, and has a bandwidth of approximately 25% of design frequency. Figure 20 is a plot of P_L and P_a over the same frequency range but with the antenna input matched to the feed system by means of a double stub tuner. The impedance match eliminates reflections at the input so $P_a = P_L$, and the absorbed power is greatly increased especially in the stopband region. An impedance match could not be attained for frequencies between 315 MHz and 405 MHz due to the limited range of the double stub tuner. The dashed portion of the curve indicates expected values of P_a had the impedance match been attained. In the power measurements, as in the impedance measurements, similar results were obtained on both structures; therefore, the results of only one are presented.

Far field E-plane patterns for both 5 gap antennas were recorded at frequencies between 450 MHz and 900 MHz. The frequency band was picked to include frequencies above and below the stopbands of both antennas. The E-plane patterns provide a means of comparing the two TEM-line antennas. They also provide a method for gain measurement which is

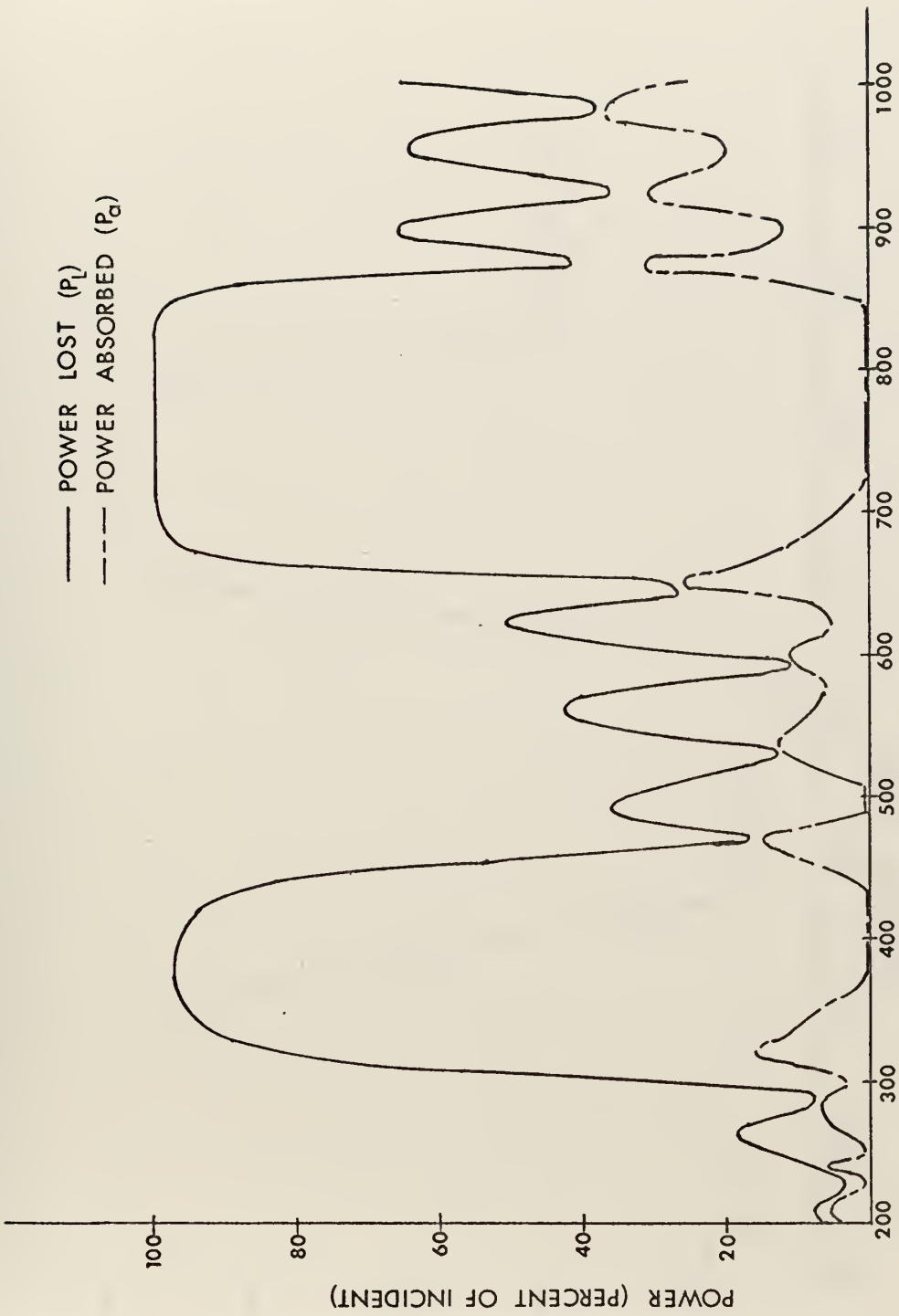

FIGURE 19. POWER IN THE FIVE-ELEMENT ANTENNA, INPUT UNMATCHED.

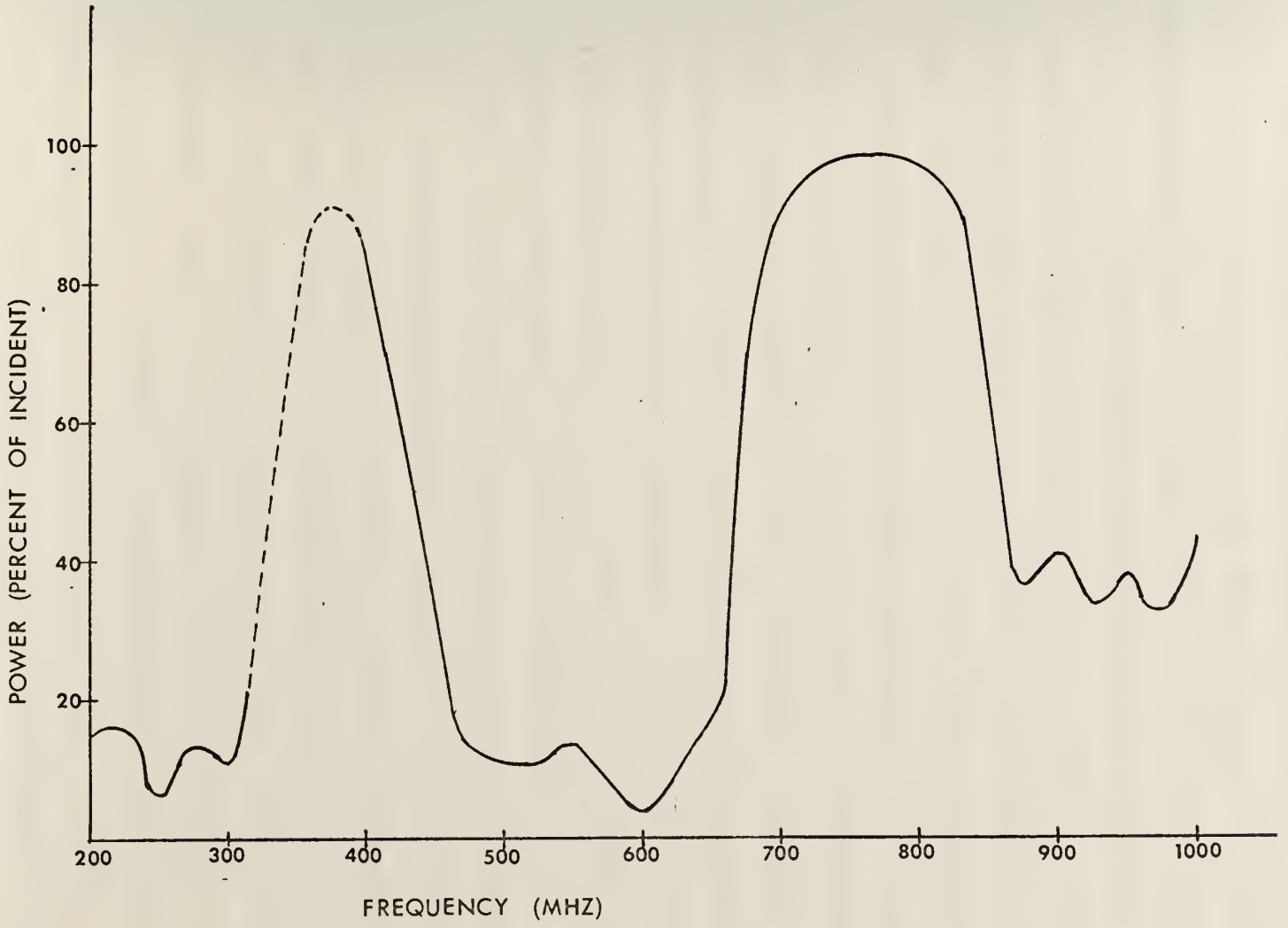

FIGURE 20. POWER IN THE FIVE-ELEMENT ANTENNA, INPUT MATCHED ($P_L=P_a$).

accomplished by comparing the received signal level of the TEM-line antenna to that of an antenna of known gain.

The experimental procedure followed for recording the pattern was to first adjust the short termination for maximum received signal and then employ a double stub tuner at the input to obtain maximum power into a 50 ohm load. After recording the TEM-line antenna pattern at each frequency the antenna was replaced by a resonant $\lambda/2$ dipole and the gain comparison was made. Due to the very narrow bandwidth of the matched condition and the difficulty of attaining the match it was necessary to have indicators at the antenna when tuning and matching at each frequency. This was accomplished by using a lightweight wide-range microwave receiver which provided both meter and CRT indication of input signal strength. The receiver also included the attenuators employed in the gain comparisons.

The recorded antenna patterns are shown in Figures 21-30. The antenna and pattern orientation can be described by using the spherical coordinate system. The antenna was positioned in the $\theta = 90^{\circ}$ plane with the feed on the $\phi = 0^{\circ}$ axis and termination on the $\phi = 180^{\circ}$ axis. Thus, broadside radiation is at $\phi = 90$ degrees, backfire at angles less than 90 degrees, and endfire at angles greater than 90 degrees. The pattern for the reference dipole shown on Figure 21b indicates the necessity of placing the antennas in the same physical location when comparing signal strengths. The unsymmetric dipole pattern is caused by reflections on the

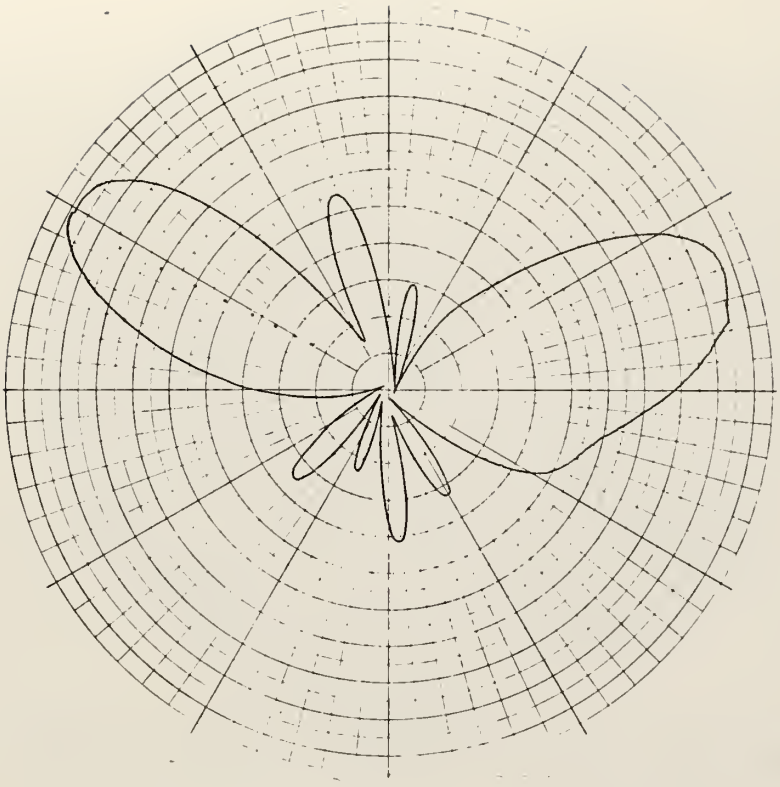

(a) 5 cm gaps, 450 MHz, 4 db below isotropic

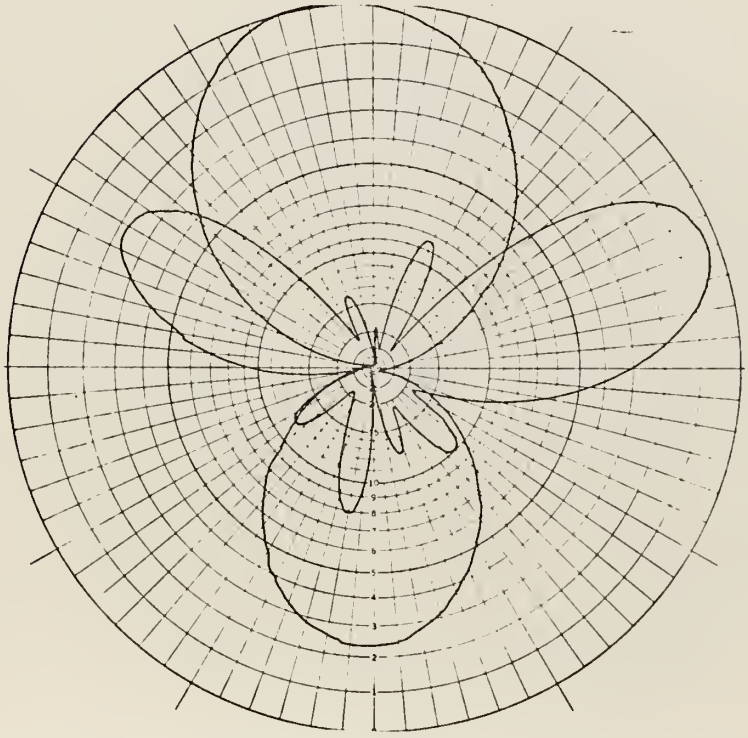

(b) 10 cm gaps, 450 MHz, 4 db below isotropic

FIGURE 21. RADIATION PATTERNS OF THE FIVE GAP ANTENNAS, (b) INCLUDES THE PATTERN OF THE RESONANT λ/2 DIPOLE.

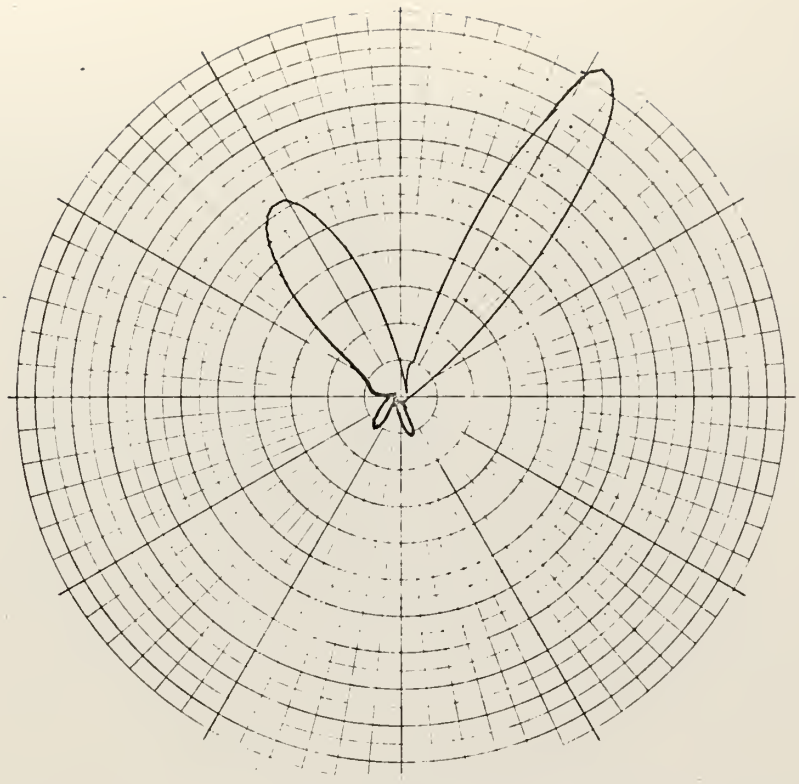

(a) 5 cm gaps, 550 MHz, 1.5 db above isotropic

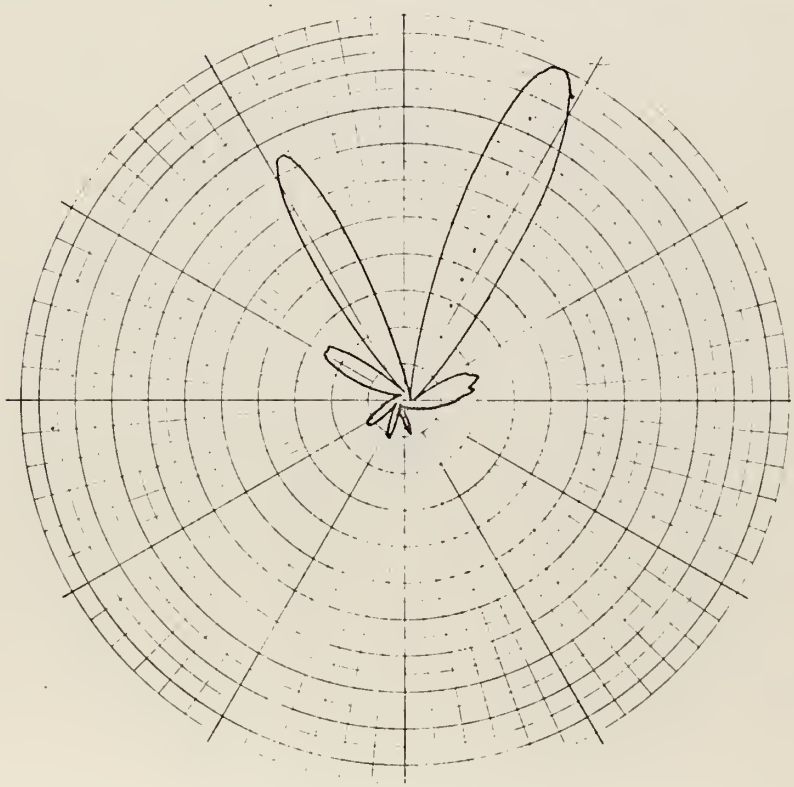

(b) 10 cm gaps, 600 MHz, 0.5 db above isotropic

FIGURE 22. RADIATION PATTERNS OF THE FIVE GAP ANTENNAS

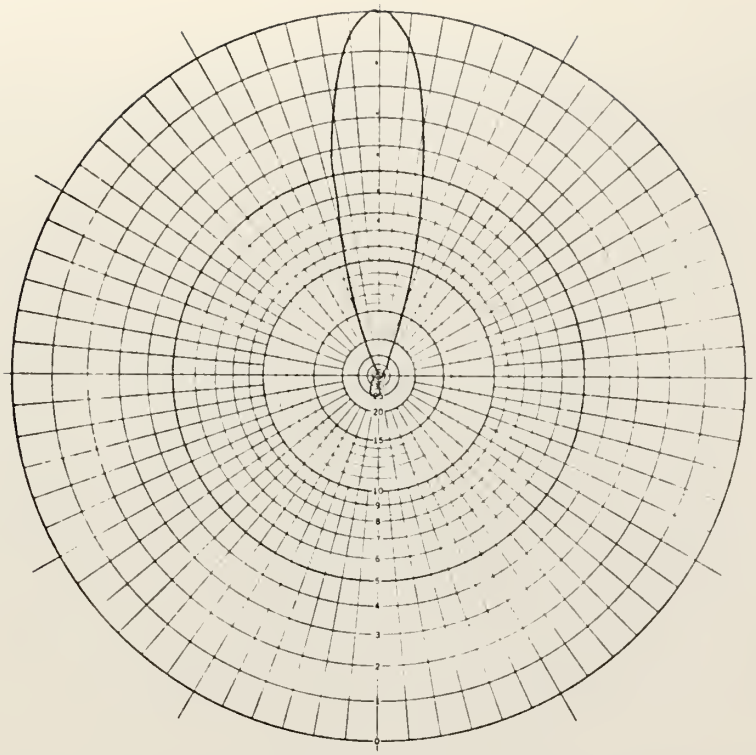

(a) 5 cm gaps, 650 MHz, 0.5 db below isotropic

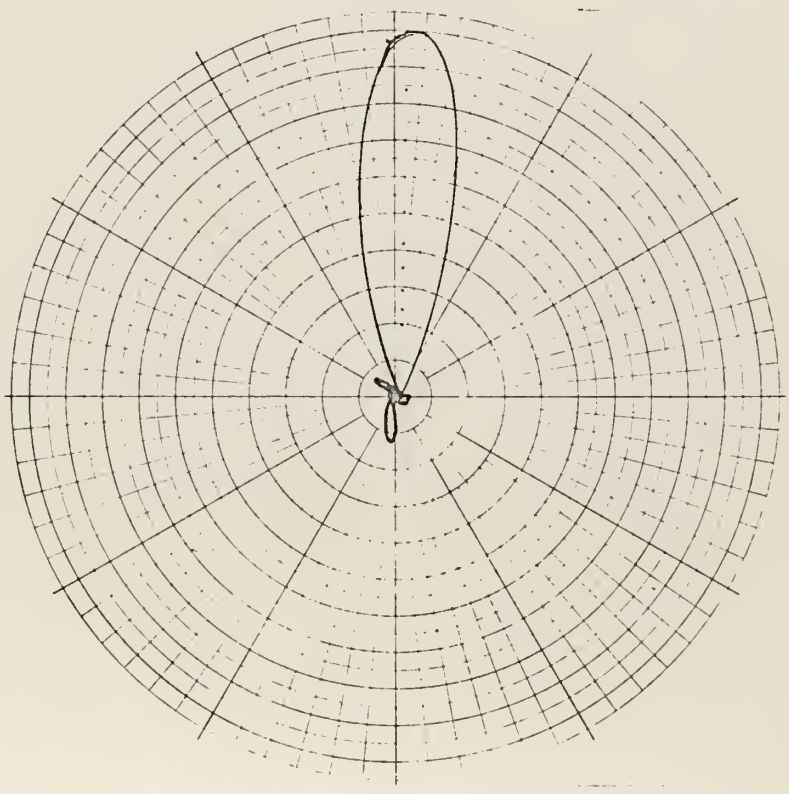

(b) 10 cm gaps, 675 MHz, 0.5 db above isotropic

FIGURE 23. RADIATION PATTERNS OF THE FIVE GAP ANTENNAS

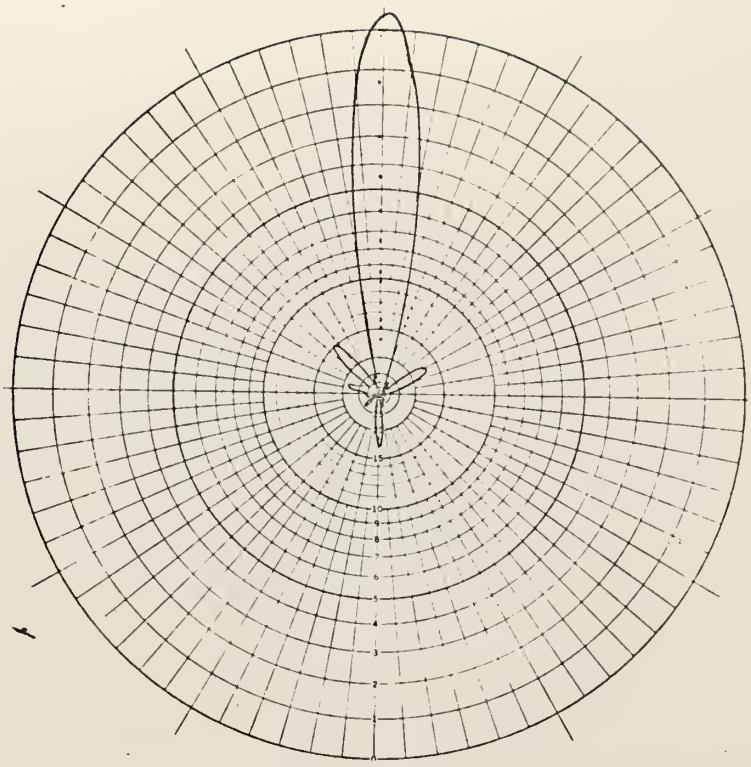

(a) 5 cm gaps, 675 MHz, 2.5 db above isotropic

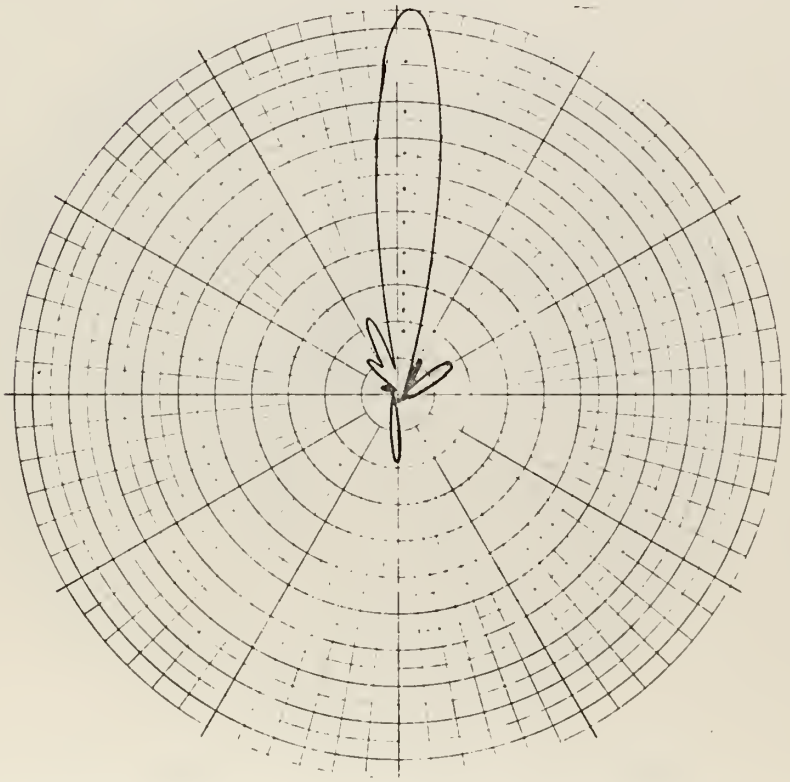

(b) 10 cm gaps, 700 MHz, 3 db above isotropic

FIGURE 24. RADIATION PATTERNS OF THE FIVE GAP ANTENNAS

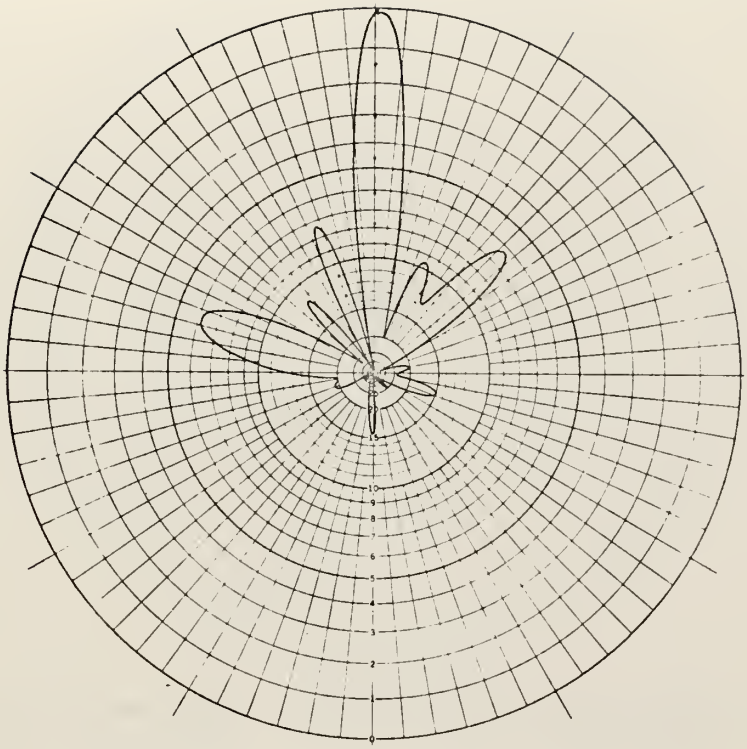

(a) 5 cm gaps, 1.5 db below isotropic

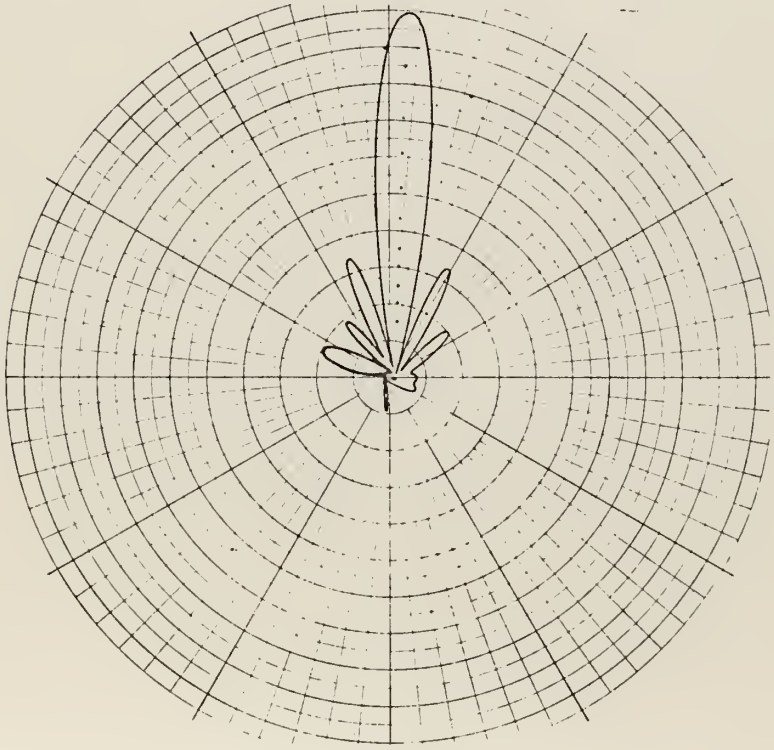

(b) 10 cm gaps, 1.5 db above isotropic

FIGURE 25. RADIATION PATTERNS OF THE FIVE GAP ANTENNAS AT 725 MHz.

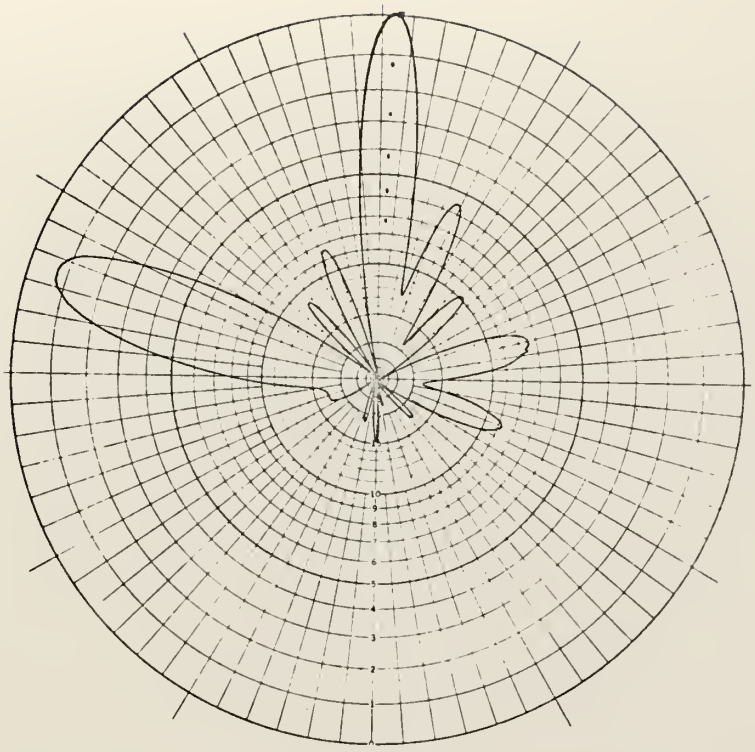

(a) 5 cm gaps, 2.0 db above isotropic

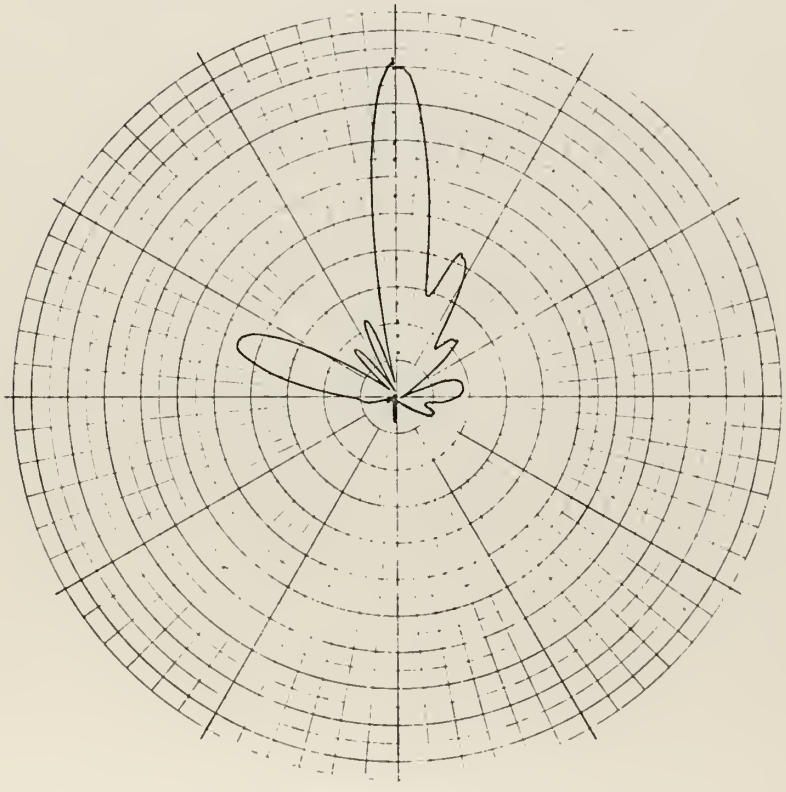

(b) 10 cm gaps, 3.5 db above isotropic

FIGURE 26. RADIATION PATTERNS OF THE FIVE GAP ANTENNAS AT 750 MHz.

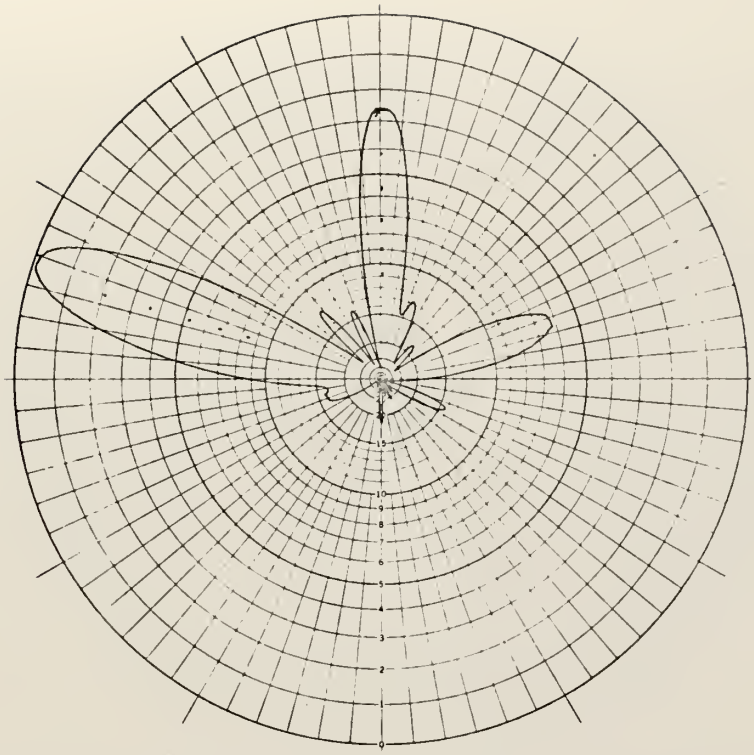

(a) 5 cm gaps, broadside lobe 6.5 db and endfire lobe 8 db above isotropic

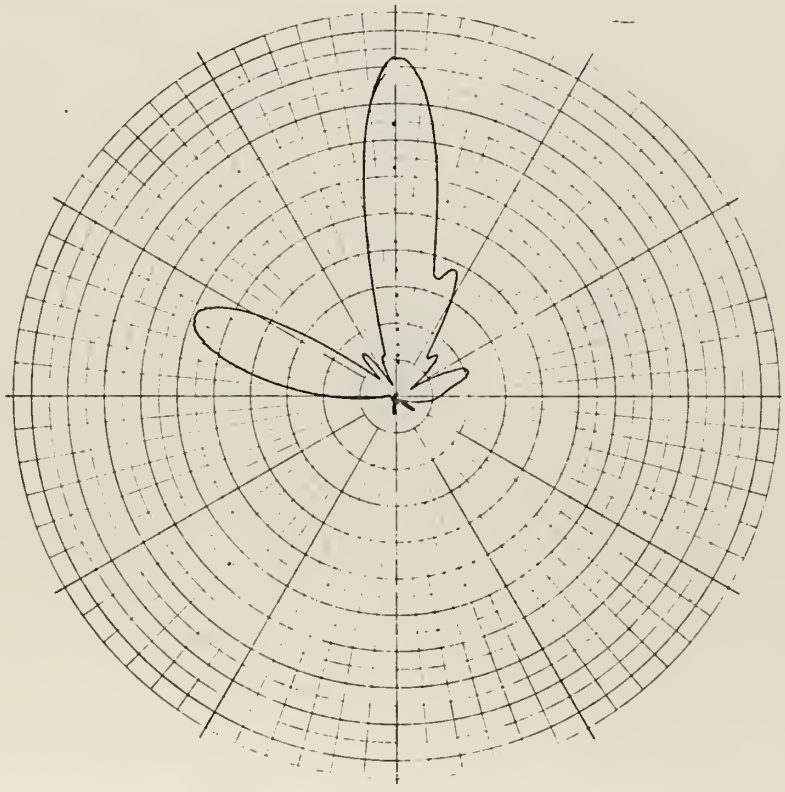

(b) 10 cm gaps, broadside lobe 8 db above isotropic

FIGURE 27. RADIATION PATTERNS OF THE FIVE GAP ANTENNAS AT 775 MHz.

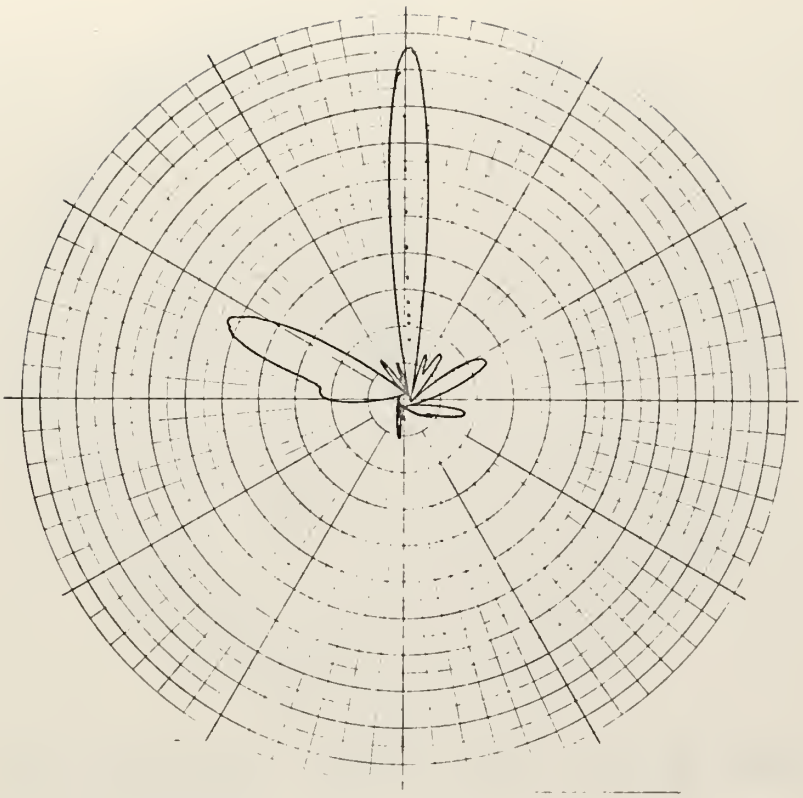

(a) 5 cm gaps, 8 db above isotropic

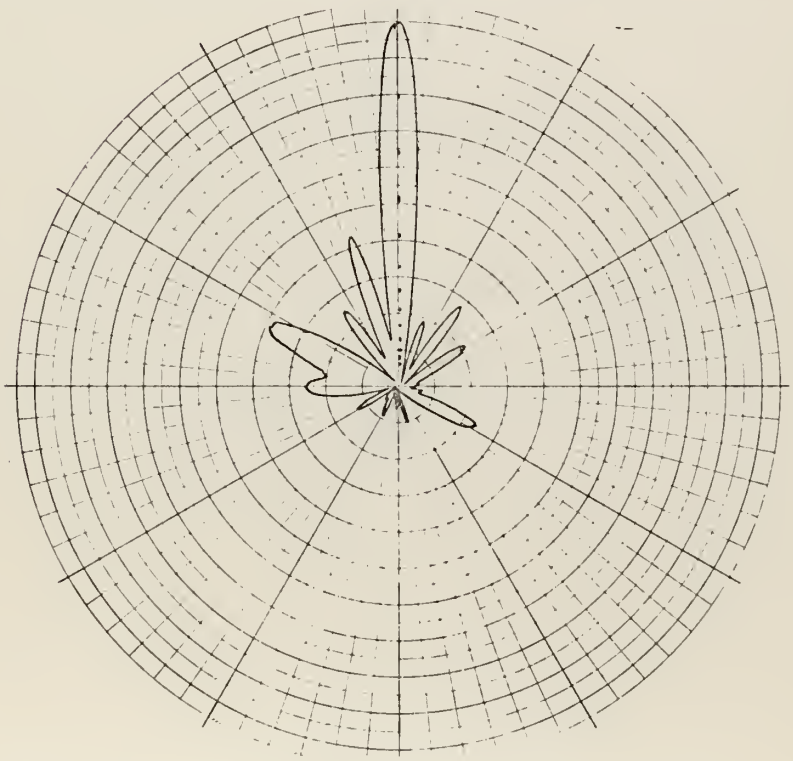

(b) 10 cm gaps, 15 db above isotropic

FIGURE 28. RADIATION PATTERNS OF THE FIVE GAP ANTENNAS AT 825 MHz.

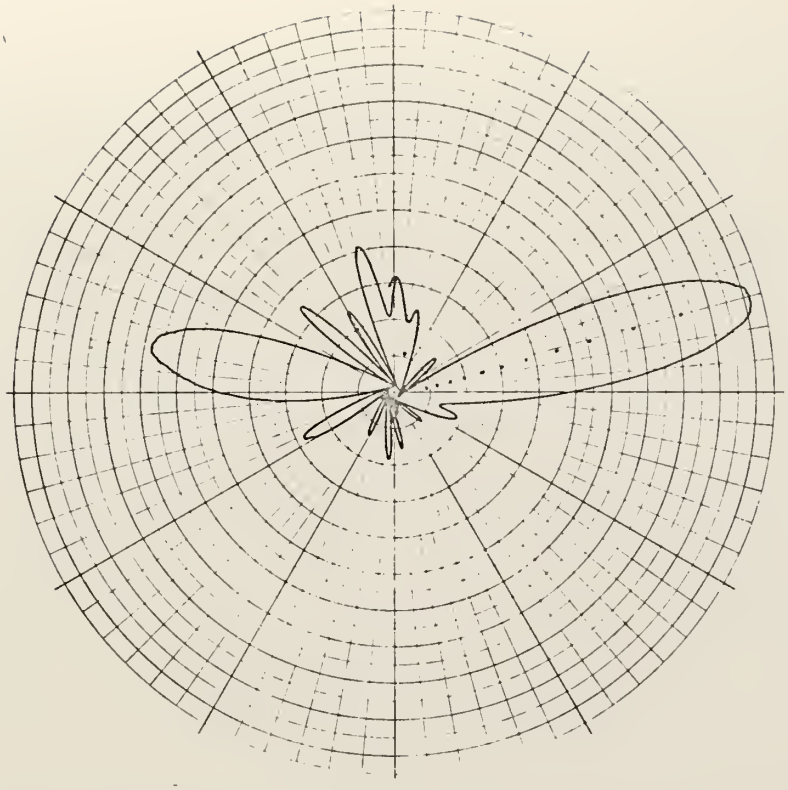

(a) 5 cm gaps, backfire lobe 12.5 db above isotropic

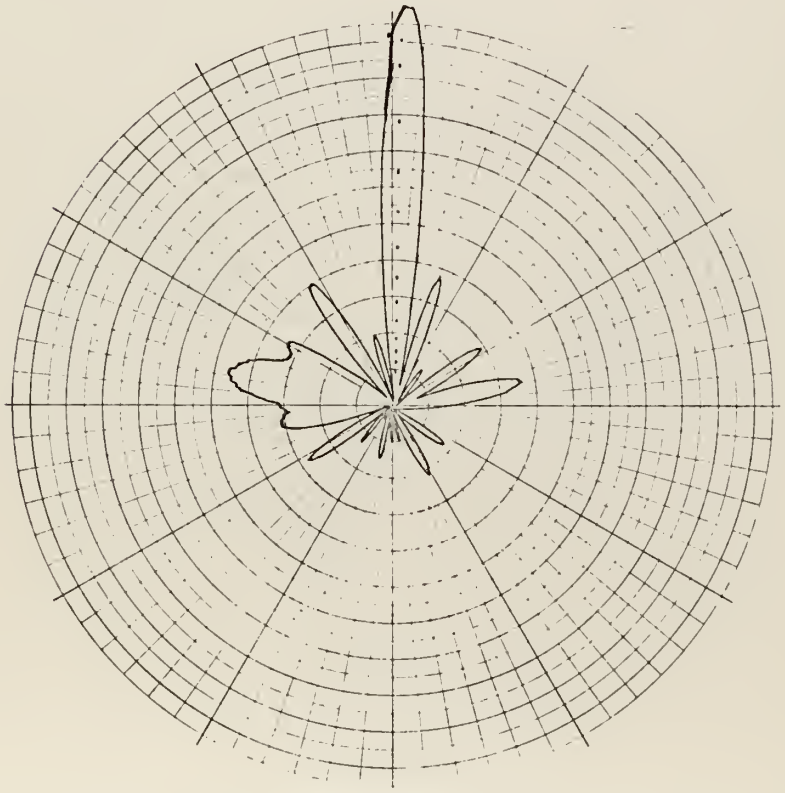

(b) 10 cm gaps, 12.5 db above isotropic

FIGURE 29. RADIATION PATTERNS OF THE FIVE GAP ANTENNAS AT 850 MHz.

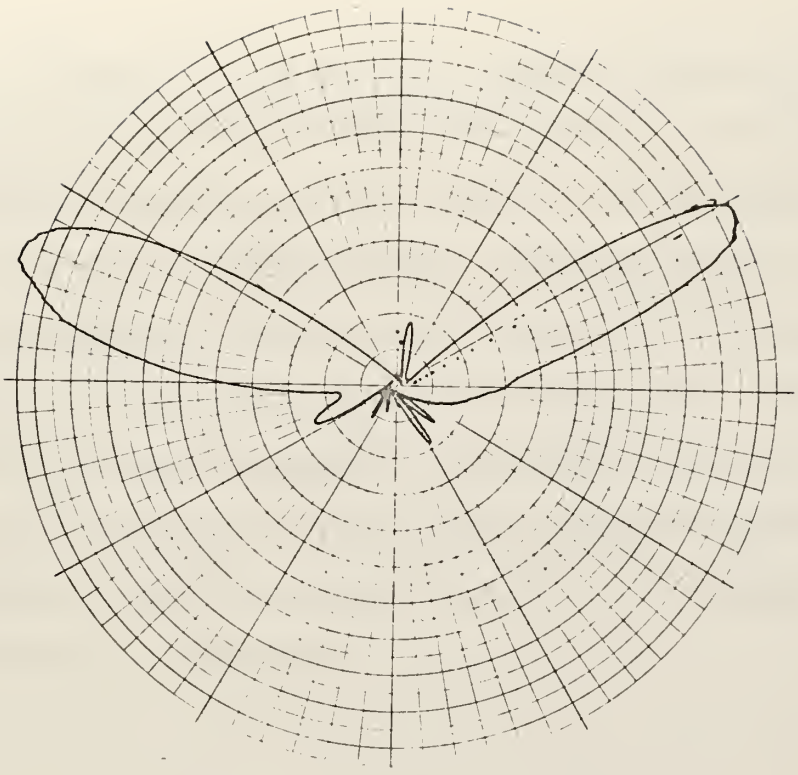

(a) 5 cm gaps, 12 db above isotropic

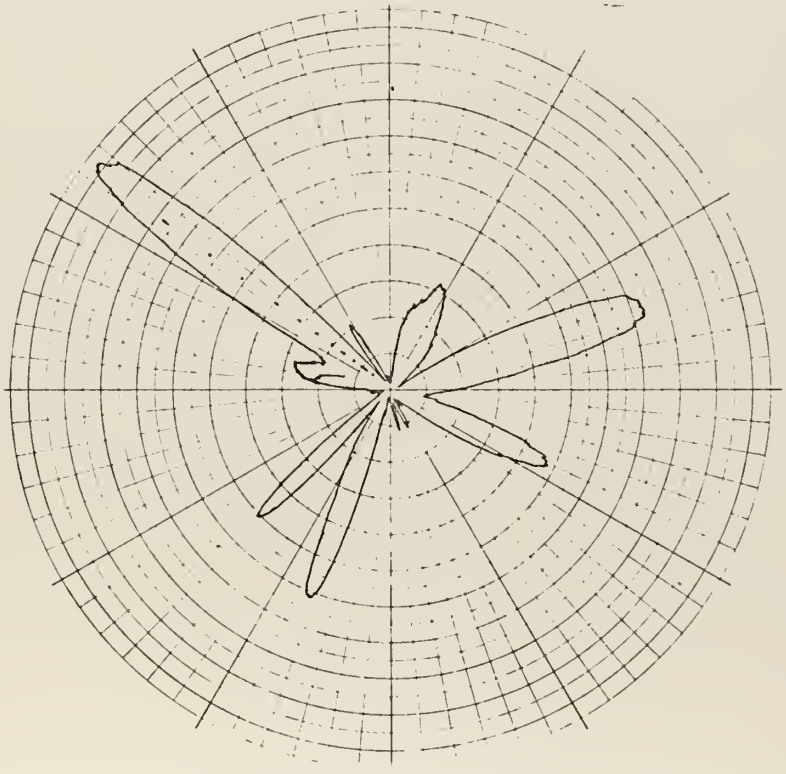

(b) 10 cm gaps, endfire lobe 3 db above isotropic

FIGURE 30. RADIATION PATTERNS OF THE FIVE GAP ANTENNAS AT 900 MHz.

antenna range. Figures 22-24 show the similar characteristics of the two structures at offset frequencies, and also demonstrate the lobe scanning characteristic as frequency is increased into the stopband region. Figures 25-30 compare the patterns and gains of the two structures from the lower stopband region to frequencies above the stopbands. The endfire lobe that becomes prominent at the mid stopband frequencies is not predicted by periodic structure theory. The theory predicts only a broadside lobe in the stopband where the structure is resonant.

III. ANALYSIS OF RESULTS

A. SINGLE GAP CHARACTERISTICS

Comparison of the calculated values of gap impedance, Figure 9, with the theoretical value shows good agreement, within 3%, between the two for gap lengths of 2.5 cm and greater. The small difference is attributed to experimental inaccuracies and the fact that the discontinuity capacitance will cause some decrease in Z_1 for all gaps.

An equation that expresses gap impedance as a function of gap parameters was desirable to facilitate prediction of gap impedance as the gap dimensions change. It was determined that the impedance equation for a parallel two wire transmission line,

$$Z_1 = \frac{\eta_o}{\sqrt{\varepsilon_r}\,\pi} \cosh^{-1}\frac{D}{\sqrt{d_1 d_2}} ,$$

can be utilized to calculate the characteristic impedance for the edge mounted gap configuration. When calculating gap impedance; D is as shown in Figure 3, η_o is the intrinsic impedance of freespace, d_1 is the diameter of the center conductor, d_2 is the thickness of the ground plane, and ε_r is the relative dielectric constant on the gap. The results indicate an accuracy to within 2% of the theoretical value.

The characteristic impedance equation enables one to predict the effect of varying the gap parameters. For example, if the ratio D/d, where $d = \sqrt{d_1 d_2}$, is increased

by a factor of 5 the gap impedance will be doubled. This increase can be accomplished simply by increasing D. A second advantage of increasing D is realized because the radiation resistance R_r increases as D^2 [2]. Thus for the configuration studied here, with D/d approximately 2 and D = 1.8 mm, if an 8mm notch were cut in the ground plane at the gap Z_1 would be doubled and R_r would be increased by a factor of twenty-five. Further, increasing D will decrease ε_r of the gap and increase the characteristic impedance even more than predicted by the dimension change.

The measurements used to determine the relative dielectric constant also show that by removing the dielectric from the center conductor, at the gap, the characteristic impedance could be increased by a factor of 1.2. Removing the dielectric does have the disadvantage of taking a great deal of protection away from the center conductor. Without the dielectric the center conductor is easily deformed and damaged causing unpredictable changes in gap characteristics; therefore, the dielectric should remain in place for protection. Desired impedance changes can be made by a simple modification of the ground plane and these modifications do not decrease the ruggedness of the structure.

The value of discontinuity capacitance, C_{DC} = 0.16pF, determined in this study compares well with the value of C_{DC} = 0.1pF determined for the surface mounted gap [2]. The higher value was expected because the dielectric was left

on the center conductor for this study, and the dimensions of the coax are much smaller than those used in the surface mount study [2].

Comparison of the gap capacitance values in Table I with the value of C_{DC} explains the decreased characteristic impedance of the smaller gaps. For example consider the 10cm gap where the capacitance is increased by a very small percentage by the addition of C_{DC} and the 0.65cm gap where the capacitance is increased by 77% due to the discontinuity cpacitance. Since impedance varies inversely with capacitance the increase in total capacitance, due to C_{DC}, causes the reduced impedance of the smaller gaps.

B. IMPEDANCE OF THE GIVE-GAP STRUCTURE

The Smith Chart plot of input impedance versus frequency for the edge mounted TEM-line antenna shows the impedance variation to be quite similar to the flush mounted antenna investigated by Kitzerow [2]. The impedance variation was rapid with relatively small magnitude changes outside the stopband while in the stopband the change in magnitude was large, as shown in Figure 12, but the change occured at a slower rate. The process of matching the antenna input to the feeder line was effective over the entire frequency band (except where the limits of the double stub tuner were exceeded). Although effective, the match was very narrow band having a bandwidth less than one percent at all frequencies. The same narrow band situation was observed when

working with the moveable short termination. That is the bandwidth over which the input impedance of the antenna remains relatively constant is very small for a fixed short position. As has been shown, the moveable short termination is effective in changing the input impedance at frequencies outside the stopband, but has very little effect in the stopband. These conditions indicate that at stopband frequencies all of the input energy is radiated or dissipated by the structure, and outside the stopband considerable energy is transmitted through the antenna. The power measurements made under matched conditions bear out these facts.

C. RADIATION CHARACTERISTICS OF THE FIVE-GAP STRUCTURE

The determination of the power absorbed by the antenna was the area of particular interest in the power measurements. The absorbed power as measured includes power dissipated by radiation from the antenna and ohmic losses on the structure. In this study no attempt has been made to separate the two or to determine values of gap radiation resistance or ohmic loss resistance. As previously stated it was assumed that the radiation resistance can be determined by the expressions derived by Kitzerow [2] for the surface mounted antenna. A comparison of the behavior of the two dissipation mechanisms is meaningful because it will show that the ohmic loss remains essentially constant, over the frequency range considered, while the radiation loss

will increase significantly over the same frequency range. The ohmic loss resistance of the gap depends on gap construction and increases as $f^{1/2}$ due to skin effect [10]; thus, the loss resistance increases only by a factor of 2 over the frequency range used. The radiation resistance, as determined for the surface mount antenna [2,3], increases as f^4; thus, an increase of approximately 600 is realized over the frequency range. This shows that as frequency increases and the absorbed power increases the additional energy is in fact being radiated and not lost as heat on the structure. The behavior of the dissipation mechanisms indicates that the antenna efficiency or gain will increase with frequency. This fact is borne out by the gain measurements.

A comparison of the two curves for P_a, Figures 19 and 20, indicates the real effect of and requirement for the impedance match. In the stopband the absorbed power increased from a measured value of zero to a value of 99% when going from an unmatched to a matched condition. And as stated a large portion of the energy is dissipated through radiation, thus verifying the stopband as the preferred operating region.

The results obtained on the two structures were similar with one exception. The stopband of the antenna with 10cm gaps was shifted up in frequency by 50MHz. The shift can be explained by the change in the phase velocity v_p on the structure. As described for the single gap v_p is greater on the gap than on the feeder coax due to the decrease in

ε_r. Therefore, as the gaps get longer and the feeder sections get shorter the overall phase velocity of the structure increases shifting the frequency of the visible region [3]; and since the stopband occurs in the center of the visible region it too is shifted.

Analysis of the far field radiation patterns shows that in general both structures perform as predicted by results from the previous studies and the theory developed for the surface mounted TEM-line antenna. For example the dual beam lobe scanning characteristic of the short terminated antenna is observed at frequencies below the stopband. The broadside lobe which persists through the entire stopband is relatively wide, 30° at the 3db point, at the lower frequencies but narrows down to about 10° at the upper edge of the stopband. The two lobes that appear at low grazing angles at frequencies just above the stopband, Figure 29a, are due to the second mode or second space harmonic [3,4]. Traveling wave antenna behavior as depicted on a Brillouin diagram [3,4] indicates that the second mode will enter the visible zone at approximately 860 MHz for the structure investigated here. The second space harmonic lobes scan in the same manner as the first mode lobes do at the lower frequencies. At frequencies above the stopband the 10cm gaps are longer than $\lambda/4$. This violates the assumption of being electrically small and much of the theory used to analyze TEM-line structures no longer holds. The end result, as shown in Figure 30b, is that the structure ceases to radiate in a predictable manner.

There are two conditions which could produce or combine to produce the endfire lobe that occurs in the stopband region. The most probable cause is that reflections from the impedance discontinuities form a forward traveling wave that produces the radiation beam in the $\phi = 165^{\circ}$ direction. The second condition is that when the magnitude of the impedance at the gaps starts to rise the capacitor dipoles begin to radiate strongly forming two beams near the ground plane [2]. Crossed field measurements made in this study indicate that the field due to the capacitor dipole is too weak to produce a lobe having the strength of the endfire lobe; therefore, the conditions can combine to form the stronger lobe as shown in Figure 27a. In that pattern the backfire lobe is due to the capacitor dipole radiation and the endfire lobe is produced by combining the effects of the traveling wave and the capacitor dipoles.

In general the structures provided low gain, 4db below isotropic at the lower frequencies, with the gain increasing significantly to a maximum of 15db above isotropic at the upper edge of the stopband. At the frequencies where maximum gain occurs the side lobes are only 3 to 4db below the main lobe. The observed increase in radiated power strongly supports the predicted rapid increase in radiation resistance and efficiency as frequency increases.

Comparison of the gain characteristics of the two structures shows quite similar results on both with the maximum gain attained from the structure having the larger gaps.

As has been shown the structure with 10cm gaps ceases to function as a radiator at frequencies where the gap length is greater than one-quarter wavelength. The larger gaps can be employed if maximum gain is required and if the frequency will not exceed the stopband range. A more consistent radiator is realized if the gaps are small enough that the $\lambda/4$ criterion is never exceeded.

Analysis of the experimental results for the two arrayed structures indicates that the edge mounted TEM-line antenna behaves much like the surface mounted version; therefore, the use of the equivalent circuits and equations developed for the surface mounted antenna is justified. The equivalent circuit as shown in Figure 7 is adequate to account for radiation, structural losses, and impedance variations. Computer simulation done in the surface mount study [2] shows the circuit to be a good model of the structure. The equivalent circuit used in this study also supports the trends established by both Layl [5] and Patak [12] in their analysis of the single gap; however, it indicates that a slightly more complicated circuit than either predicted is necessary to describe the antennas behavior.

IV. CONCLUSIONS AND RECOMMENDATIONS

A. SINGLE GAP

The geometry of the gap lends itself well to the transmission line model and therefore this appears to be the best approach to the investigation of the gap. The impedance is easily measured, the discontinuity capacitance is readily determined, and the model provides a means of accurately predicting changes as the gap dimensions and configurations vary. The effect of mutual coupling was not considered when determining the impedance of a single gap. In his study of the surface mount version, Kitzerow [2] determined that the mutual coupling was approximately one ohm for a spacing of one-quarter wavelength. That value is assumed here because of the correlation between the two types of gaps; therefore, the mutual coupling can be neglected when determining the single gap impedance.

Further study of the single gap should be directed toward verifying the effect of mutual coupling for the edge mounted antenna. Gaps constructed from coax of different characteristic impedance should be investigated to verify predicted changes in gap characteristic impedance. Another area of particular interest for future study is the overall effect of notching the ground plane at the gap.

B. ARRAYED STRUCTURE

The wide variation in input impedance indicates that the input must be matched to get energy onto the antenna. The high rate of impedance variation and the narrow bandwidth of the match condition present considerable problems in extending the bandwidth of the antenna to a useful range. One method of extending the bandwidth or tuning the antenna is by adjusting the position of a moveable short termination. This may be accomplished either mechanically by physically moving the short or electrically by means of a varactor or some similar technique.

Further study should be directed toward extending the bandwidth of the antenna either by methods suggested here or by some means of dynamic impedance transformations at the antenna input.

The s-parameter technique employed provides a straightforward method of determining the power absorption characteristics of the TEM-line antenna. The results of the power measurements lead to two significant conclusions; first, the structure must be matched at the input and second, the stopband region is the most efficient region for operation. Further study should be conducted to determine how the absorbed power is divided between radiation and ohmic loss on the structure and thereby determine efficiency as a function of frequency. Another area for future study is the use of more gaps on longer structures to determine how radiation efficiency varies with changes in these parameters.

The maximum gain of 15db above isotropic measured in this study is higher than any gain previously reported on a TEM-line antenna. Copeland [4] reported a maximum gain of 12.3db above isotropic on a 5 gap surface mounted TEM-line antenna designed for operation at frequencies between 1 and 2 GHz. The 5 cm gap is believed to be the optimum size gap for TEM-line antennas designed for 750 MHz because the antenna with 10 cm gaps ceases to function at the higher frequencies and the gains of both antennas were nearly the same.

The particular application of any TEM-line antenna will dictate the portion of the frequency band that the antenna must operate in. For example, if an installation requires a pattern free of sidelobes the antenna will have to operate in the lower part of the stopband and gain must be sacrificed for clean patterns. On the other hand if sidelobes cause no problems the antenna can be operated in the upper end of the stopband where maximum gain is attained. Other available modes of operation are the lobe scanning mode below the stopband and the second space harmonic lobe scanning mode above the stopband. As can be seen, there are many modes for many applications of this simple low profile antenna.

In final conclusion, the edge mounted TEM-line antenna was found: to be easily constructed, to display rapid variation of input impedance with frequency, to have moderate gain, to operate in several different modes in a given frequency band, and to fit a variety of applications on aircraft, missiles, and even ship installations.

LIST OF REFERENCES

1. Agrawal, P. K., and others, "Analysis and Design of TEM-Line Antennas", IEEE Transactions on Antennas and Propagation, Vol. AP-20, No. 5, Pp. 561-568, September 1972.

2. Kitzerow, R.A., Basic Theory of TEM-Line Antennas, MS thesis, Ohio State University, 1967.

3. Electro Science Laboratory, Department of Electrical Engineering, Ohio State University, Technical Report 2341-1, The Slotted TEM-Line Antenna - A Low Profile, Beam Scanning, Traveling Wave Antenna, by T. E. Kilcoyne, 3 April 1967.

4. Copeland, J. R., Analysis of the TEM-Line Antenna, PhD thesis, Ohio State University, 1969.

5. Layl, J. N., The Impedance Characteristics of a Coaxial TEM-Line Antenna, MS thesis, United States Naval Postgraduate School, 1972.

6. Whinnery, J. R., Jamieson, H. W., and Robbins, T. E., "Coaxial Line Discontinuities", Proceedings IRE, Vol. 32, P. 695, November 1944.

7. Hewlett-Packard Company, Application Note 77-3, Measurement of Complex Impedance, by members of the Hewlett-Packard Company staff, 1967.

8. Hewlett-Packard Company, Application Note 67, Cable Testing With Time Domain Reflectometry, by members of the Hewlett-Packard Company staff, 1968.

9. Hayt, W. H., Engineering Electromagnetics, 2d ed., Pp. 153-159, McGraw-Hill, 1967.

10. Ramo, R., Whinnery, J. R., and Van Duzer, T., Fields and Waves in Communications Electronics, Pp. 603-612, Wiley, 1967.

11. Hewlett-Packard Company, Application Note 77-1, Transistor Parameter Measurements, by members of the Hewlett Packard Company staff, 1967.

12. Patak, L. W., Admittance Characteristics of a Coaxial TEM-Line Antenna, MS thesis, United States Naval Postgraduate School, 1971.

INITIAL DISTRIBUTION LIST

		No. Copies
1.	Defense Documentation Center Cameron Station Alexandria, Virginia 22314	2
2.	Library, Code 0212 Naval Postgraduate School Monterey, California 93940	2
3.	Asst. Professor R.W. Adler, Code 52Ab Department of Electrical Engineering Naval Postgraduate School Monterey, California 93940	2
4.	A.G. Jennetti Electro-Magnetic Systems Lab. Inc. 495 Java Dr. Sunnyvale, Calif. 95288	1
5.	Librarian Ohio State University Electro-Science Lab. 1320 Kinnear Road Columbus, Ohio, 43212	1
6.	Lt. D.E. Schultz, USN 4763 51st St. San Diego, Calif. 92115	1
7.	Lt. J.N. Layl, USN 1145 Bennion St. Honolulu, Hawaii 96818	1
8.	Capt. Lowell W. Patak, USMC Rural Route 1 Stacy, Minnesota 55079	1

Security Classification

DOCUMENT CONTROL DATA - R & D

(Security classification of title, body of abstract and indexing annotation must be entered when the overall report is classified)

1. ORIGINATING ACTIVITY (Corporate author)

Naval Postgraduate School
Monterey, California 93940

2a. REPORT SECURITY CLASSIFICATION

Unclassified

2b. GROUP

3 REPORT TITLE

An Investigation into the Characteristics of the Edge Mounted Coaxial TEM-Line Antenna

4. DESCRIPTIVE NOTES (Type of report and inclusive dates)

Master's Thesis; December 1972

5. AUTHOR(S) (First name, middle initial, last name)

Dale Edward Schultz

6. REPORT DATE	7a. TOTAL NO. OF PAGES	7b. NO. OF REFS
December 1972	66	12

8a. CONTRACT OR GRANT NO.	9a. ORIGINATOR'S REPORT NUMBER(S)
b. PROJECT NO.	
c.	9b. OTHER REPORT NO(S) (Any other numbers that may be assigned this report)
d.	

10. DISTRIBUTION STATEMENT

Approved for public release; distribution unlimited.

11. SUPPLEMENTARY NOTES	12. SPONSORING MILITARY ACTIVITY
	Naval Postgraduate School Monterey, California 93940

13. ABSTRACT

The edge mounted TEM-line antenna is a lightweight, low profile, medium-gain UHF-VHF traveling wave antenna. The antenna is capable of operating in several different modes in a given frequency band. In its simplest form the antenna consists of a small diameter semi-rigid coaxial transmission line bonded to the edge of a conducting ground plane. Sections of the coax outer conductor are removed at periodic intervals to form the radiating elements.

This paper presents methods of measuring and calculating the characteristic impedance and discontinuity capacitance of a single edge mounted radiating element. Scattering parameter techniques are employed to investigate input impedance and power absorption characteristics of arrays of TEM-line elements. Far-field radiation patterns are used to determine antenna gains and compare the performance of different array configurations.

DD FORM 1 NOV 65 1473 (PAGE 1)

S/N 0101-807-6811

Security Classification

A-31408

KEY WORDS	LINK A		LINK B		LINK C	
	ROLE	WT	ROLE	WT	ROLE	WT
TEM-Line Antenna						
Low Profile Antenna						
Traveling Wave Antenna						
Periodic Structures						

141749

Thesis
S3645
c.1

Schultz
An investigation into
the characteristics of
the edge mounted coaxial
TEM-line antenna.